KTH Architecture and
the Built Environment

Models for analysis of young cast and sprayed concrete subjected to impact-type loads

LAMIS AHMED

Doctoral Thesis
Stockholm, Sweden 2015

TRITA-BKN. Bulletin 132, 2015
ISSN 1103-4270
ISRN KTH/BKN/B--132--SE

KTH School of ABE
SE-10044 Stockholm
SWEDEN

Akademisk avhandling som med tillstånd av Kungliga Tekniska högskolan framlägges till offentlig gransking för avläggande av teknologie doktorsexamen i Byggvetenskap, med inriktning mot Betongbyggnad, tisdagen den 9 juni 2015, klockan 10:00 i sal D2, Lindstedtsvägen 5, Stockholm.

Abstract

The strive for a time-efficient construction process naturally put focus on the possibility of reducing the time of waiting between stages of construction, thereby minimizing the construction cost. If recently placed concrete, cast or sprayed, is exposed to impact vibrations at an early age while still in the process of hardening, damage that threatens the function of the hard concrete may occur. A waiting time when the concrete remains undisturbed, or a safe distance to the vibration source, is therefore needed. However, there is little, or no, fully proven knowledge of the length of this distance or time and there are no established guidelines for practical use. Therefore, conservative vibration limits are used for young and hardening concrete exposed to vibrations from e.g. blasting.

As a first step in the dynamic analysis of a structure, the dynamic loads should always be identified and characterized. Here it is concluded that impact-type loads are the most dangerous of possible dynamic loads on young and hardening concrete. Shotcrete (sprayed concrete) on hard rock exposed to blasting and cast laboratory specimens subjected to direct mechanical impact loads have been investigated using finite element models based on the same analysis principles. Stress wave propagation is described in the same way whether it is through hard rock towards a shotcrete lining or through an element of young concrete. However, the failure modes differ for the two cases where shotcrete usually is damaged through loss of bond, partly or over larger sections that may result in shotcrete downfall. Cracking in shotcrete due to vibrations only is unusual and has not been observed during previous in situ tests. The study of shotcrete is included to demonstrate the need of specialized guidelines for cases other than for mass concrete, i.e. structural elements or concrete volumes with large dimensions in all directions.

Within this project, work on evaluating and proposing analytical models are made in several steps, first with a focus on describing the behaviour of shotcrete on hard rock. It is demonstrated that wave propagation through rock towards shotcrete can be described using two-dimensional elastic finite element models in a dynamic analysis. The models must include the material properties of the rock and the accuracy of these parameters will greatly affect the results. It is possible to follow the propagation of stress waves through the rock mass, from the centre of blasting to the reflection at the shotcrete-rock interface. It is acceptable to use elastic material formulations until the strains are outside the elastic range, which thus indicates imminent material failure. The higher complexity of this type of model, compared with mechanical models using mass and spring elements, makes it possible to analyse more sophisticated geometries. Comparisons are made between numerical results and measurements from experiments in mining tunnels with ejected rock mass and shotcrete bond failure, and with measurements made during blasting for tunnel construction where rock and shotcrete remained intact. The calculated results are in good correspondence with the in situ observations and measurements, and with previous numerical modelling results. Examples of preliminary recommendations for practical use are given and it is demonstrated how the

developed models and suggested analytical technique can be used for further detailed investigations.

The modelling concept has also been used for analysis of impact loaded beams and concrete prisms modelled with 3D solid elements. As a first analysis step, an elastic material model was used to validate laboratory experiments with hammer-loaded concrete beams. The laboratory beam remained un-cracked during the experiments, and thus it was possible to achieve a good agreement using a linear elastic material model for fully hardened concrete. The model was further developed to enable modelling of cracked specimens. For verification of the numerical results, earlier laboratory experiments with hammer impacted smaller prisms of young concrete were chosen. A comparison between results showed that the laboratory tests can be reproduced numerically and those free vibration modes and natural frequencies of the test prisms contributed to the strain concentrations that gave cracking at high loads. Furthermore, it was investigated how a test prism modified with notches at the middle section would behave during laboratory testing. Calculated results showed that all cracking would be concentrated to one crack with a width equal to the sum of the multiple cracks that develop in un-notched prisms. In laboratory testing, the modified prism will provide a more reliable indication of when the critical load level is reached.

This project has been interdisciplinary, combining structural dynamics, finite element modelling, concrete material technology, construction technology and rock support technology. It is a continuation from previous investigations of the effect on young shotcrete from blasting vibrations but this perspective has been widened to also include young, cast concrete. The outcome is a recommendation for how dynamic analysis of young concrete, cast and sprayed, can be carried out with an accurate description of the effect from impact-type loads. The type of numerical models presented and evaluated will provide an important tool for the work towards guidelines for practical use in civil engineering and concrete construction work. Some recommendations on safe distances and concrete ages are given, for newly cast concrete elements or mass concrete and for newly sprayed shotcrete on hard rock.

Keywords: Young concrete · Shotcrete · Rock · Impact-type vibration · Finite element method · Fracture mechanics model · Crack width

Sammanfattning

Strävan efter en tidseffektiv byggprocess fokuserar på ett naturligt sätt på möjligheten att minska väntetidetider mellan byggetapper, vilket minimerar byggkostnaden. Om nyligen placerad betong, gjuten eller sprutad, utsätts för vibrationer av stöttyp vid tidig ålder då härdningsprocessen fortfarande pågår, finns risk för skador som hotar att försämra funktionen hos den fullhårdnade betongen. Därför behövs en väntetid där betongen förblir ostörd, eller ett säkert avstånd till vibrationskällan. Det finns däremot liten eller ingen fullt vedertagen kunskap om längden på detta avstånd, eller tidsperiod, och det finns heller inga fastställda riktlinjer för praktisk användning. Därför används idag konservativa gränsvärden för ung och hårdnande betong som utsätts för vibrationer från t.ex. sprängning.

Som ett första steg i en dynamisk analys av en struktur ska de dynamiska lasterna alltid identifieras och karakteriseras. För de typer av dynamiska belastningar som kan verka på ung och hårdnande betong är effekten från laster av stöttyp den allvarligaste. De två fallen med sprutbetong på hårt berg utsatt för sprängning och gjutna laboratorieprovkroppar utsatta för direkt mekanisk stötlast har undersökts med hjälp av finita elementmodeller baserade på samma analysprinciper. Spänningsvågornas utbredning beskrivs på samma sätt oavsett om det är genom hårt berg mot en sprutbetongyta eller genom ett konstruktionselement av ung betong. Dock är brottmoderna olika för de två fallen, där sprutbetong oftast skadas genom vidhäftningsbrott, delvis eller över större sektioner vilket kan leda till nedfall av sprutbetong. Sprickbildning i sprutbetong på grund av enbart vibrationer är ovanligt och har inte observerats under tidigare fältförsök. Studien av sprutbetong har medtagits för att påvisa behovet av specialiserade riktlinjer för andra fall än för massiva betongkonstruktioner, dvs. strukturella element eller betongvolymer med stora dimensioner i alla riktningar.

Inom detta projekt genomförs arbetet med att utvärdera och föreslå analysmodeller i flera steg, först med fokus på att beskriva beteendet hos sprutbetong på hårt berg. Det visas att vågutbredning genom berget mot sprutbetongen kan beskrivas med hjälp av tvådimensionella elastiska finita elementmodeller i en dynamisk analys. Modellerna måste inkludera bergmaterialets egenskaper och riktigheten hos dessa parametrar kommer att ha stor påverkan på resultaten. Det är möjligt att följa utbredningen av spänningsvågor genom bergmassan, från sprängningens centrum till reflektion vid gränsskiktet mellan sprutbetong och berg. Tillräcklig noggrannhet ges med elastiska materialformuleringar, tills töjningar överskrider det elastiska området vilket indikerar förestående materialbrott. Den högre komplexiteten hos denna typ av modell, jämfört med mekaniska modeller med massor och fjäderelement, kommer att möjliggöra analyser med avancerade geometrier. Jämförelser görs här mellan numeriska resultat och mätningar från experiment i gruvtunnlar, med utstött bergmassa och vidhäftningsbrott, och med mätningar gjorda under sprängning för tunnelbygge, där berg och sprutbetong förblev intakta. De beräknade resultaten är i god överensstämmelse med fältförsöken och med tidigare presenterade numeriska resultat. Exempel på preliminära

rekommendationer för praktiskt bruk ges och det visas hur föreslagen analysteknik och de utvecklade modellerna kan användas för kommande detaljerade undersökningar.

Modelleringskonceptet har också använts för analys av stötbelastade balkar och betongprismor som har modellerats med solida 3D element. I en första analys användes en elastisk materialmodell för att validera ett laboratorieexperiment med hammarbelastade betongbalkar. Laboratoriebalken förblev oförstörd under provningen och därmed var det möjligt att uppnå god överensstämmelse med en linjärelastisk materialmodell för fullt hårdnad betong. Modellen utvecklades ytterligare för att möjliggöra modellering av spruckna provkroppar. För kontroll av de numeriska resultaten valdes en tidigare genomförd serie laboratorieförsök med hammarbelastade mindre prismor av ung betong. En jämförelse mellan resultaten visade att laboratorieresultaten kan återges numeriskt och att provkropparnas fria vibrationsmoder och egenfrekvenser bidragit till spänningskoncentrationer som gav sprickbildning vid höga belastningar. Dessutom har det undersökts hur en sådan provkropp, modifierad med skåror i mittsektionen, skulle bete sig under samma laboratorieförsök. Beräkningsresultat visade att all sprickbildning då skulle koncentreras till en spricka med en bredd som är lika med summan av de flera sprickor som utvecklas i en oskårad provkropp. I laboratorietester kommer den modifierade provkroppen att ge en mer tillförlitlig indikation på när den kritiska skade- och belastningsnivån nås.

Projektet har varit tvärvetenskapligt och kombinerat strukturdynamik, finit elementmodellering, betongmaterialteknik, konstruktionsteknik och bergförstärkningsteknik. Det är en fortsättning från tidigare undersökningar av effekten på ung sprutbetong från sprängningsvibrationer, men detta perspektiv har vidgats till att även omfatta ung gjuten betong. Resultatet består av rekommendationer för hur dynamisk analys av ung betong, gjuten och sprutad, kan genomföras med en korrekt beskrivning av effekten från laster av stöttyp. Den typ av numeriska modeller som presenterats och utvärderats kommer att vara ett viktigt verktyg för arbetet med att ta fram riktlinjer för praktisk användning vid anläggnings- och betongbyggnadsarbete. Några rekommendationer för säkerhetsavstånd och minimiåldrar ges, för nygjutna betongelement eller massiva betongkonstruktioner och för nyligen applicerad sprutbetong på hårt berg.

Nyckelord: Ung betong · Sprutbetong · Berg · Stötar och vibrationer · Finita elementmetoden · Brottmekaniksk modell · Sprickbredd

Preface

The work has been carried out at the KTH Royal Institute of Technology, Division of Concrete Structures. The study was made possible through financial support from BeFo, Rock Engineering Research Foundation and SBUF, the Development Fund of the Swedish Construction Industry. Support to the first part of the Project also came from Formas, The Swedish Research Council for Environment, Agricultural Science and Spatial Planning. The support is gratefully acknowledged.

I would like to express my sincere thanks and gratitude to my supervisor Professor Anders Ansell and assistant supervisor Ph.D. Richard Malm for their guidance, assistance, supervision, and encouragement during the term of this project.

I also wish to express my grateful thanks to the staff of the laboratory at Department of Civil and Architectural Engineering at KTH for providing all the necessities for executing the laboratory works.

Appreciation thanks to Professor Jonas Holmgren for his support, to all my colleagues and especially thanks to my brother *Ahmad* and his family.

Stockholm, June 2015

Lamis Ahmed

List of appended papers

The thesis contains the following research papers, referred to in the text by their roman numerals:

I. Ansell A, Ahmed L. Impact load vibrations on young concrete. Submitted to Structural Concrete, 2015.

II. Ahmed L, Ansell A. Laboratory investigation of stress waves in young shotcrete on rock. Magazine of Concrete Research 64(10):899-908, 2012.

III. Ahmed L, Ansell A. Structural dynamic and stress wave models for the analysis of shotcrete on rock exposed to blasting. Engineering structures 35:11-17, 2012.

IV. Ahmed L, Ansell A, Malm R. Finite element simulation of shotcrete exposed to underground explosions. Nordic Concrete Research 45:59-74, 2012.

V. Ahmed L, Ansell A. Vibration vulnerability of shotcrete on tunnel walls during construction blasting. Tunnelling and Underground Space Technology 42:105–111, 2014.

VI. Ahmed L, Ansell A, Malm R. Numerical modelling and evaluation of laboratory tests with impact loaded young concrete prisms. Submitted to Materials and Structures, 2015.

Paper I was mainly written by Ansell, with Ahmed contributing to the literature search and evaluation of the results. For Papers II, III and V, Ahmed carried out the laboratory investigation, performed the numerical calculations and wrote the paper together with Ansell. The numerical calculations in Paper IV and VI were done by Ahmed with contributions from Malm. The evaluation of the results and writing of the paper was done by Ahmed together Ansell and Malm.

As complement to the above papers, the following additional reports and conference papers have been published during the project:

Ahmed L. Models for analysis of shotcrete on rock exposed to blasting. Licentiate thesis. Stockholm: KTH Royal Institute of Technology; 2012.

Ahmed L. Laboratory simulation of blasting induced bond failure between rock and shotcrete. Stockholm: Rock Engineering Research Foundation. BeFo report 116, 2012.

Ahmed L, Ansell A. Behaviour of sprayed concrete on hard rock exposed to vibration from blasting operations. Proceeding of 7th International Conference on Sprayed Concrete. Sandefjord: The Norwegian Society of Graduate Technical and Scientific Professionals, Tekna; 2014.

Ahmed L, Ansell A. Experimental and numerical investigation of stress wave propagation in shotcrete. In: XXI Symposium on Nordic Concrete Research and Development. Hämeenlinna: Nordic Concrete Research; 2011.

Ahmed L, Ansell A. A comparison of models for shotcrete in dynamically loaded rock tunnels. Proceedings of the 3rd international conference on engineering developments in shotcrete. Queenstown: Australian Shotcrete Society and the American Shotcrete Association; 2010.

Contents

Chapter 1

Introduction

A criterion for how severe impact induced vibrations that can be allowed to reach young and hardening concrete is needed for efficient civil engineering projects, e.g. casting of concrete foundations on ground, tunnelling or other underground constructions. Striving for a more time-efficient construction process naturally focuses on the possibilities of reducing the times of waiting between stages of construction, which will lead to a reduced construction cost.

1.1 Background

Recently placed, young and hardening concrete is vulnerable to high intensity vibrations of impact-type that may cause a reduction of its strength in the hardened state. Vibration stress waves will propagate through a concrete volume and depending on the existence of free and restrained boundary surfaces, compressive and tensile stresses will appear. Since the compressive strength of concrete is higher than the tensile strength, damage due to tensile cracking of the concrete matrix may occur during the hardening process. The damaging mechanisms inside curing concrete subjected to impact-type vibrations are complicated and little is known about their effects. Therefore, conservative vibration limits have been used for hardening concrete exposed to vibrations, in many cases leaving engineers to conduct empirical investigations and testing without any clear and reliable guidelines given. This is reflected in the differences that exist between limits specified in different national standards and handbooks, often given with allowed peak particle velocity (PPV) at a certain point where damage protection is required.

The allowable PPV levels vary strongly as the concrete hardens and its strength increases. Also, the maximum PPV that can be allowed close to recently placed concrete depends on geometry, construction type, and load situation and may be fundamentally different if e.g. mass concrete or shotcrete (sprayed concrete) is studied. The damage caused in shotcrete on rock is often the result of bond failure while damage on aboveground concrete structures from e.g. underground blasting is due to structural dynamic response problems. Therefore, it is necessary to determine reliable safety limits for impact vibration in relation to concrete type, concrete ages, dynamic characteristics, etc. However, to establish reliable guidelines comparison between in situ or laboratory observations and measurements with finite element modelling results are needed to gain the understanding of the causes of possible damage in young concrete exposed to severe vibrations.

This project is a continuation from previous investigations of the effect on young shotcrete from blasting vibrations. In situ tests were conducted underground in a Swedish mine [9], as a first step towards reliable guidelines for how close, in time and distance, to young and hardening shotcrete blasting can be allowed. The in situ tests were evaluated using comparisons with results from numerical models [8, 10-11]. These were based on elastic stress wave theory and structural dynamics and with relatively small computational effort made it possible to compare a large number of calculations with various combinations of input data. The first phase of this project has also been presented in a licentiate thesis [2] and its appended papers, here also included as Papers II, III and IV, on models for analysis of shotcrete on rock exposed to blasting. The previously used engineering models were compared and evaluated through calculations and comparisons with existing data. Results from a non-destructive laboratory experiment were also used to provide test data for the models. A more sophisticated, dynamic finite element model was also developed and tested using the numerical program Abaqus [119]. This allows modelling of more complex geometries and provides more detailed analysis results. The second phase, presented here together with the conclusion from the first part of the project, also studies the effect from vibrations on young and hardening cast concrete. The developed and tested finite element model is here also used with a non-linear material formulation that can simulate concrete cracking. The case with shotcrete on hard rock is thus a special case that can be analysed with similar methods as cast concrete elements and volumes, but for other geometries and material properties. The most important difference is here the failure modes, where cast concrete develops cracks while shotcrete often fails due to loss of bond to the rock.

1.2 Early age concrete

There are several alternative definitions of '*early age concrete*', used differently within the various fields of concrete engineering and research. A review of common terms and their corresponding time spans is presented by Ansell and Silfwerbrand [4], here summarized in Table 1.1. The term '*young concrete'* often refers to recently placed concrete, being 0 – 12 hours old while '*old concrete*' is concrete older than one week. For ages between young and old, the term '*intermediate age concrete*' is used. With reference to the hardening process, '*initial setting*' corresponds to the time when concrete is no longer workable and has very little or no slump while '*final setting*' indicates the time at which the concrete begins to harden, but when still no measurable strength can be observed, [98].The American Concrete Institute [1] defines '*early age of concrete*' as the period after final setting during which properties are changing rapidly. This definition is similar to that for '*green concrete*', defined as concrete that has undergone final setting but not fully hardened. These two definitions imply that the concrete has reached final set but has not gained much strength. The early strength of concrete or mortar is usually [1] given at various times during the first 72 hours after placement, for '*early age concrete*' often defined as concrete between setting and approximately 24–72 hours old, [29]. Research findings indicate that the setting period represents the interval of the most rapid hydration, followed by a period of reduced hydration activity, i.e. induction. The beginning of the setting period is not mainly defined since it depends on many factors, i.e. type of cement, water/cement ratio, temperature, etc. However, e.g. the Swedish Concrete handbook [128] states that the setting period starts after 3–5 hours from the first contact between water and cement. Through the setting period, a major portion of the cement hydrates and then solidifies which normally continues up to 24–72 hours. In the present study, '*early age concrete*' is used to denote concrete less than 72 hours old. For very

early ages the term '*young concrete*' is used, which here represents the period from first contact between cement and water up to 12 hours of age. The most critical concrete age is often assumed to be within 3–14 hours after casting, but is believed to vary with the type of concrete and curing conditions, see [4 and 64]. Concrete ages are often also defined with respect to equivalent time, which depends on temperature and thus the rate of hardening. The measure is then often the compressive strength and workability of the hardening concrete. An example is given by Fjellström et al. [42] who define '*fresh concrete*' as concrete that can be placed and vibrated without damage to the cement structure, i.e. similar to the definition by Byfors [29] in Table 1.1. The following time period is referred to as a '*surface finishing period*' which is the time between initial and final setting when final work can be made to the concrete surface. The third period is the '*hardening period*' that typically begins from a compressive strength of around 0.5 MPa. However, it should be remembered that apart from curing and placing temperatures, concrete material properties such as damping characteristics, use of admixtures, types and number of binders, i.e. cement and fly ash [133], are also important for when young concrete is as most sensitive to vibration damage.

Table 1.1: A compilation of terminology for young and early age concrete, from [4].

Term	Concrete ages	Definition given by:
Fresh concrete	concrete before setting	Byfors [29]
Green concrete	freshly placed, ≤24 hours	Hulshizer and Desai [63]
Young concrete	0–12 hours	Akins and Dixon [3]
Early age concrete	between setting and app. 1–3 days	Byfors [29]
Intermediate age concrete	12 hours – 7 days	Akins and Dixon [3]
Almost hardened concrete	app. 1–3 days to 28 days	Byfors [29]
Old concrete	≥7 days	Akins and Dixon [3]
Hardened concrete	≥28 days	Byfors [29]

There are often practical problems associated with testing of young and hardening concrete. Material properties such as compressive strength, tensile strength and modulus of elasticity are difficult to measure on concrete younger than 12 hours. For younger concrete it may be difficult to remove casting moulds for stiffness or strength measurement, [73]. Despite this, the effects of vibration on early age concrete have been studied through a number of tests carried out using widely different methods. A variety of methods for applying vibration loads to concrete test specimens has been used. These vary from hammering the specimens to produce impact vibration, or vibrating the specimens on a shaker table, to subjecting the specimens to ground vibrations at a construction site. The latter is often done by placing concrete specimens adjacent to sources of construction-induced vibration such as rock-blasting, pile-driving, heavy traffic, or machine vibrations, as further explained in [Paper I]. There is no agreement on how vibration damage to the concrete should be defined and detected. Measurement of only the compressive strength of vibration-exposed and later hardened concrete specimens might not reveal the full effects of the shock vibration applied [75]. There might also be difficulties in detecting damage from vibrations in early age concrete since e.g. hairline cracks are difficult to observe with the naked eye. However, early

investigations such as the study by Esteves [41], relied on visual inspection to detect surface cracks as a sign of vibration damage to the concrete, [36 and 61]. Due to this, large variations in the results between experimental studies can be seen demonstrating that more clear failure criteria such as reduction in compressive or tensile strength should be used. The vibration resistance of concrete depends more on tensile than on compressive strength, and vibration damages also show mainly in the form of cracking and reduction in tensile strength, [73]. However, because tensile strength is more difficult to test than compressive strength, especially for young concrete, many researchers therefore omitted to investigate the tensile strength. One reason is that reinforced concrete is often designed in the cracked state making tensile strength less important with respect to impact vibrations in such cases, see e.g. Hulshizer and Desai [63]. Thus, due to the lack of detailed knowledge of how vibrations cause damage to early age concrete there are no generally accepted methods for estimating these limits. In some tests, despite shock vibrations up to what was believed to be a very high PPV, no damage to the concrete specimens had been detected. In most of these tests, the threshold vibration intensity that would cause vibration damage had not yet been reached and the results obtained were only safe PPV levels that would not cause vibration damage, and no ultimate vibration limits. Although the tensile strength is relatively low during the first 24 hours after casting, it has been suggested that within the first 2 hours, i.e. before initial set, young concrete is able to withstand PPV up to 100 mm/s, [63 and 104], and may also benefit from the re-vibration [4].

1.3 Shotcrete

Shotcrete is concrete projected pneumatically onto a surface, using either the dry mix or the wet mix method. The latter has been widely used for tunnelling work in hard rock and its flexibility in the choice of application thickness, material compositions (e.g., fibre content), output capacity and fast early strength development makes shotcrete a material well suited for rock support. Most construction work in underground rock involves the use of explosives for excavation work. Rock surfaces are often secured with shotcrete immediately after the excavation blasting to prevent fallout of smaller blocks. Therefore, shotcrete must often be able to carry loads and withstand disturbances early after spraying, [27]. However, movements in the rock mass and especially vibrations from blasting during tunnelling may cause damage that threatens the performance of the hardened shotcrete, [1]. Damage may lead to full or partial de-bonding between shotcrete and rock that could affect the efficiency of the rock support and the overall safety of e.g. a tunnel or underground opening. The relation between the strength growth for important material parameters such as modulus of elasticity and tensile strength is important for the capacity to resist vibrations, [27]. Material data for cast concrete is often used for analyses involving shotcrete. However, even though the basic material compositions are similar, the method of placement, the use of set accelerators and other additives gives shotcrete unique material properties. The underground temperatures and humidity also affect the strength growth ratio that differs from that of cast concrete.

In tunnelling, the use of shotcrete is often restricted near the area where blasting takes place, due to the risk of vibration damage, as demonstrated in Figure 1.1. An important example is the driving of two parallel tunnels that requires coordination between the two excavations so that blasting in one tunnel does not, through vibrations, damage temporary support systems in the other tunnel prior to installation of a robust, permanent support, see Figure 1.2. Similar problems also arise in mining where the grid of drifts in a modern mine is dense. This means

that supporting systems in one drift are likely to be affected by vibrations in a neighbouring drift. Thus, to be able to excavate as much ore volume as possible, there is a need to know how close, in time and distance, to shotcrete blasting can be allowed. Previous studies show that shotcrete without reinforcement, also as young as a couple of hours, can withstand vibration levels as high as 500−1000 mm/s while sections with loss of bond and ejected rock appear for vibration velocities higher than 1000 mm/s [5]. Similar measurements, based on in situ experiments conducted in Japan [97], showed that vibration velocities of 700 mm/s cracked the observed shotcrete lining. The response of steel fibre-reinforced and steel mesh-reinforced shotcrete linings subjected to blasts was investigated in a Canadian mine [135]. It was observed that the shotcrete remained attached to the rock surface for vibration levels up to 1500–2000 mm/s, with only partial cracking observed in the shotcrete.

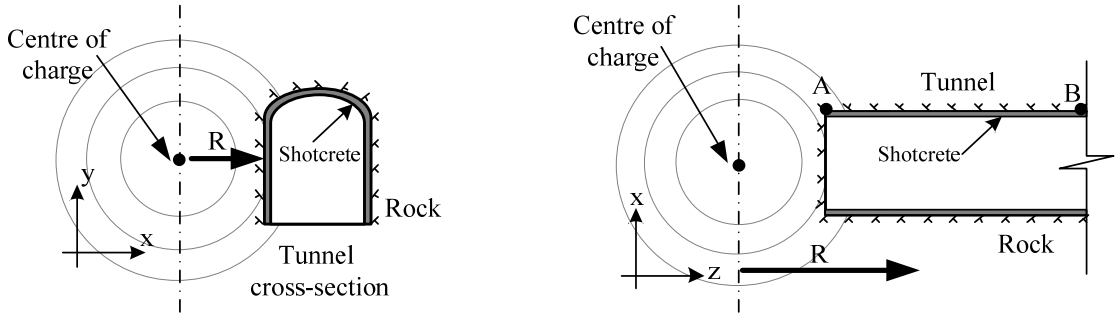

Figure 1.1: Examples of stress waves in rock; (left) tunnel profile and (right) tunnel plane, from [2].

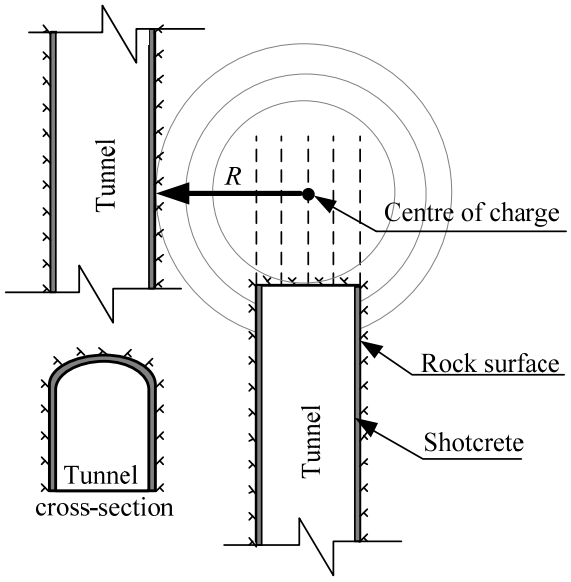

Figure 1.2: Construction of two parallel tunnels, redrawn from [67].

1.4 Aims and goals

This project aims at suggesting numerical methods suitable for analysis of young and hardening concrete subjected to impact-type vibrations. Focus is on how impact-type vibrations damage young concrete and when impact is the most relevant load case. One

important research question is how to perform a dynamic analysis that realistically captures the characteristics of the load, the structural response of the analysed concrete element or volume and indicates concrete damage caused by the load. The main goal is to recommend a finite element based analysis model, describe how the impact load can be practically applied and how the resulting stress wave propagation can be modelled and described numerically. The project also includes a comparison between the effects of different types of vibrations. Important factors and material properties that must be accounted for in the analysis will be identified, discussed and commented.

One further objective within the project is to assess how the suggested type of analysis models can be used for the case with young shotcrete (sprayed concrete) on rock walls subjected to blasting. One important question here is how the behaviour of cast and sprayed concrete differs, with respect to failure modes, damage types, critical ages, etc. The study of shotcrete is included to demonstrate the need of specialized guidelines for cases other than for mass concrete, i.e. structural elements or concrete volumes with equal dimensions in all directions. The use of set accelerators in shotcrete also gives different time spans for the age when the young material is particularly sensitive to disturbance. The goal is here to give recommendations for how criteria for maximum vibration levels should be formulated, depending on the case studied.

As part of the conclusions from the project recommendations will also be given. These will cover the identified need of further research and practical aspects of further numerical investigations within the field. Comments on how to use and interpret existing guidelines and standards for practical civil engineering work will be given, together with suggestions for improved guidelines. The outcome of the project will be an increased understanding of the failure mechanisms involved in young concrete vibration damage and will also provide researchers with an analysis tool for calculation of results to be compared with results obtained in laboratory and in situ environments. The practical recommendations given will be an important contribution to a more efficient, safe and economical construction process with concrete close to impact vibration sources.

1.5 Outline of thesis

The thesis is a compilation containing six papers, presenting the majority of the results from the project. Paper I is a state-of-the art report on the field of impact vibrations on young and hardening concrete. A laboratory test program is presented in Paper II, giving results from measurements on stress wave propagation in concrete beams and their effect on the bond to young shotcrete. Papers III and IV investigate and compare a number of numerical analytical models for dynamic analysis. Based upon these results, a finite element approach and model is suggested. A case study based on measurements during tunnelling is presented in Paper V, comparing earlier in situ measurements with finite element results for shotcrete on tunnel walls adjacent to blasting. The use of non-linear concrete material models is investigated in Paper VI, where numerical results are compared with an earlier laboratory test. The papers are summarized and their combined contents supported by additional information given in the thesis part of the compilation. The eight chapters of the thesis are organized as follows:

Chapter 1 - Presents background and objectives of the thesis project.

Chapter 2 - Gives a summary of relevant load types that cause impact-type vibrations.

Chapter 3 - Is a compilation of guidelines and recommendations given in the Papers I-VI.

Chapter 4 - Summarizes the in situ and laboratory investigations that are used for comparison and verification of the analytical and numerical models tested.

Chapter 5 - Describes the models here used for dynamic analysis.

Chapter 6 - Gives a short summary of the six appended papers.

Chapter 7 - Presents recommendations for further analytical modelling work, use and interpretation of presented vibration guidelines and suggestions for future research and investigations.

Finally, chapter 8 presents conclusions from the project, based upon the papers, and the comments and discussions in the thesis part.

Chapter 2

Impact-type vibrations

In this chapter a summary of relevant load types that cause impact-type vibrations is given. First, the characteristics of dynamic loads are commented. Then follows by a discussion of important classes of loads that are mild or severe types of impacts but also of traffic loads that are usually of nonimpact-types. However, the latter is included to provide background and motive for focusing on short duration vibration loads of high magnitudes, i.e. impact-type vibrations.

2.1 Dynamic load types

Vibrations acting on structures and constructions can have a variety of different external sources, including industrial, construction and transportation activities. An important first step in the dynamic analysis of a structure is to identify and characterize the dynamic loads that may occur. For concrete structures, this is important already from the time of casting. According to [13], a vibration may be classified as continuous with magnitudes that vary or remain constant with time, impulsive such as impact and shocks or intermittent, with the magnitude of each event being either constant or varying with time. All types of high magnitude vibrations may cause damage to young concrete but in most practical cases continuous vibrations are often of low magnitudes. Such vibrations, for example from machinery, steady road traffic, construction activities with e.g. tunnel boring machines, have therefore not been covered in this study. However, traffic vibrations will be commented in the following since several studies are published and the results are often referred to when vibration limits are discussed.

Examples of typical impulsive and intermittent vibration loads, expressed as function of strain rate, are given in [6] and here shown in Figure 2.1. Strain rate is the rate of change in strain of a material with respect to time and for e.g. an axially compressed bar it can be calculated as the speed at which the ends approach each other divided by the original length of the bar. From the figure, it can be seen that the highest strain rates occur from blasting that can generate strain rates within the range of 100 – 1000 s^{-1}. It should be noting that traffic vibrations, but also collisions, are associated with relatively low dynamic load levels. The higher load classes correspond to direct explosions, missile impacts, etc. Also, the material strength of concrete increases with strain rate and a dynamic increase factor (DIF), the ratio of the dynamic to the static value is often used for this representation. The elastic modulus is also strain rate dependent, which is usually assumed to be due to a decrease in internal micro

cracking for increasing strain rates. As seen in the compilations of test results presented in Figures 2.2 – 2.3 there is a little effect on the DIF at low strain rates, for both compressive and tensile loading. As a comparison it should be noted that in the CEB-FIP Model Code [65] a static compressive load is defined as corresponding to a strain rate of $3 \cdot 10^{-5}$ s^{-1}. However, from strain rates above approximately $1s^{-1}$ there is a sudden increase in DIF, which is more obvious to the tensile strength. See e.g. [79, 84 and 103] for a thorough discussion of the subject, where also all the references given in Figures 2.2 – 2.3 are listed and commented. The load cases studied within this project generate strain rates that reach strain rates of around $1s^{-1}$. It should be noted that for blast loads the strain rate depends on the distance between the centre of the explosion and the point of observation, with increasing rates for decreasing distance. The strain rate levels in Figure 2.1 refer to close proximity blasting while blasting in situ during construction work usually generates strain rates in the same range as from pile driving, i.e. around $1s^{-1}$ [114]. It should also be noted that there are few investigations of the strain rate dependence of very young and hardening concrete. For the numerical examples presented in the following it is therefore assumed that any possible increase in material strength and elastic modulus due to strain rate effects is already accounted for and included in the material parameters used.

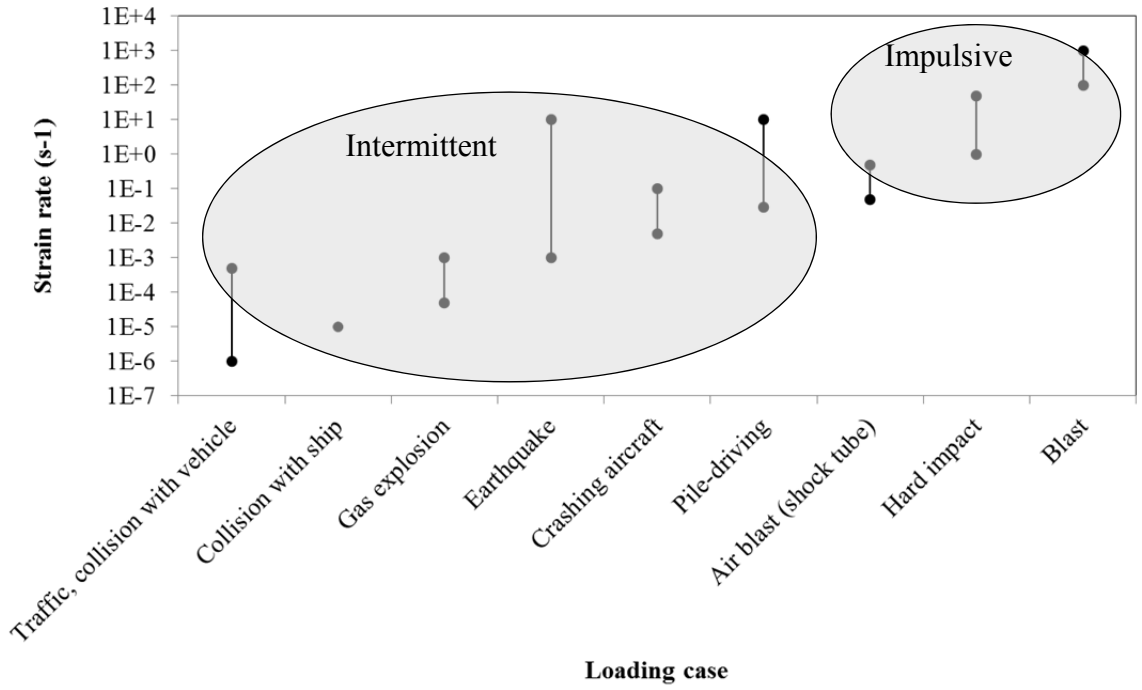

Figure 2.1: Approximate strain rate associated with various cases of loading, from [6].

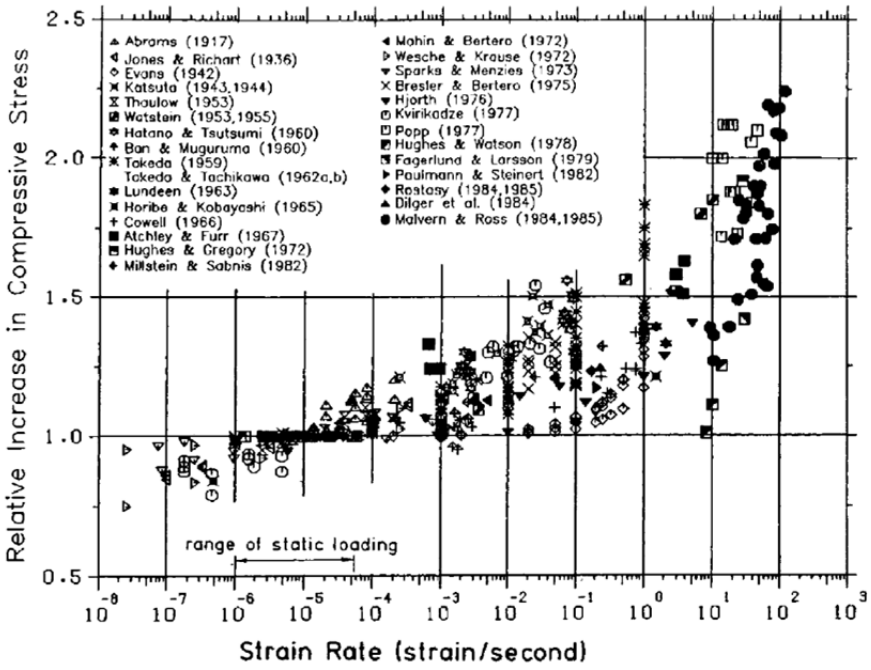

Figure 2.2**:** Strain rate effects on the concrete compressive strength, from [19].

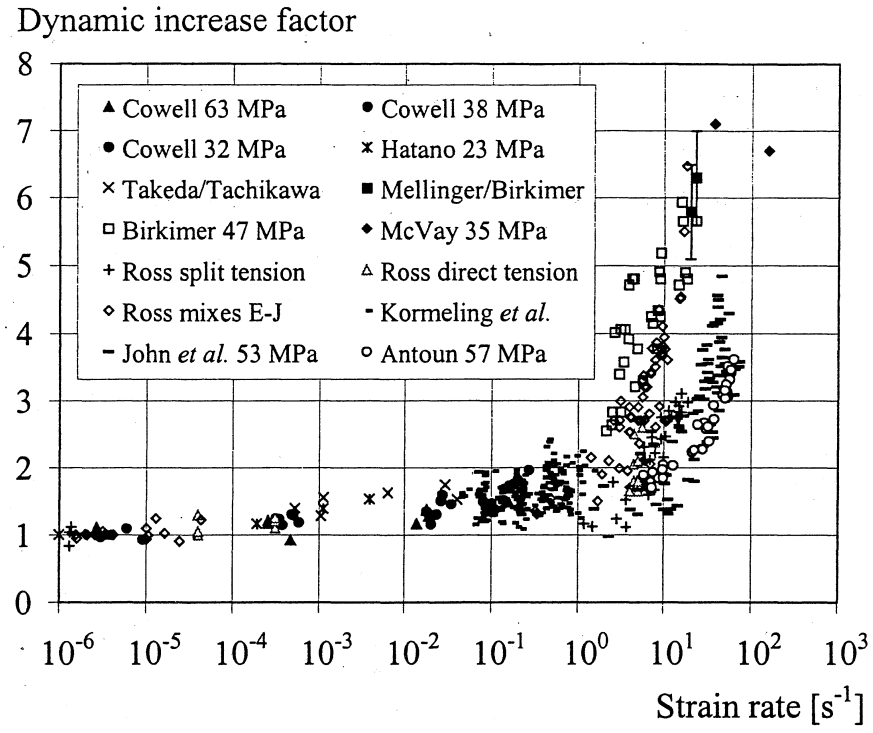

Figure 2.3: Strain rate effects on the concrete tensile strength, Reproduced from [84], based on [87].

The frequency content of dynamic loads is also an important parameter so an alternative classification of dynamic load on concrete structures is based on to the frequency contents and the amplitude, as seen in Figure 2.4. Generally, it can be seen that blast loading is associated with high frequencies and amplitudes, i.e. PPV whereas both traffic and pile driving vibrations are associated with low frequencies but with and high and low amplitudes, respectively. A comparison with the recommended maximum vibration velocities for young and hardening concrete is given in [Paper I], and here later in Chapter 3, gives values up to 180 mm/s, which is much lower than the range of 500-2000 mm/s representative for blasting in Figure 2.4. However, it should be noted that shotcrete damage has been documented to occur at 500-1000 mm/s, see [2 and 9], and that undamaged cast concrete subjected to 1800 mm/s of vibrations has been observed, see [76]. The frequency ranges given in Figure 2.4 should be seen as typical average values that may show large variation depending on ground type or structural stiffness. It should be noted that the compilation in [Paper I] gives the frequency range for e.g. traffic vibration and pile driving as 1-100 Hz and for ground-borne blasting vibrations as 1-300 Hz. From the in situ measurements with shotcrete on hard rock [9] frequencies within the range of 150-2400 Hz were recorded.

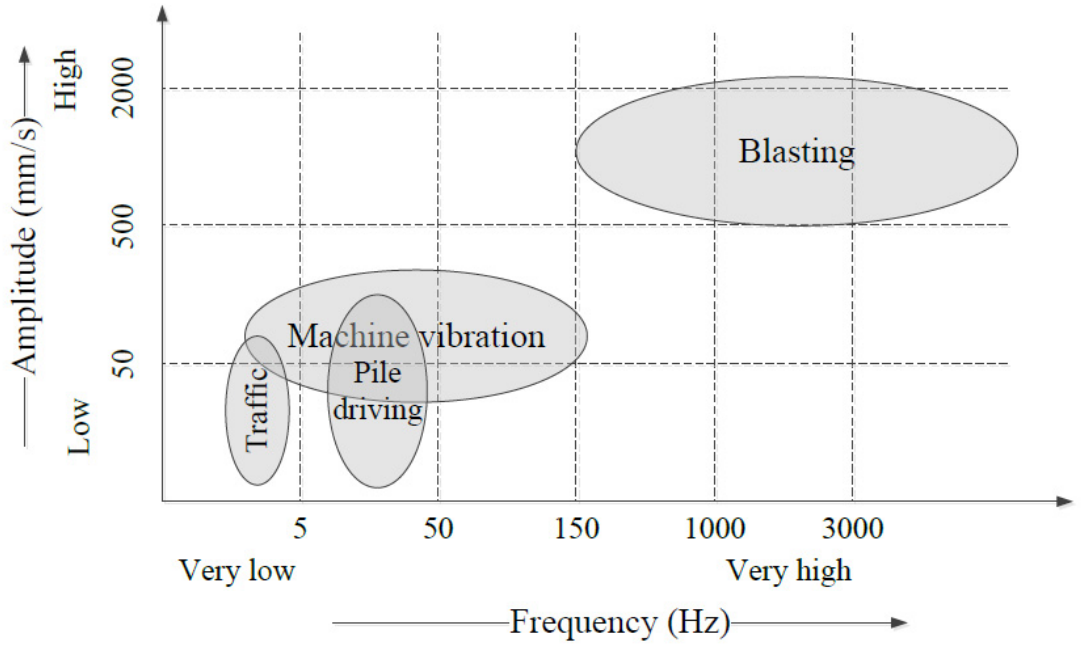

Figure 2.4: Frequencies and amplitudes for different dynamic loads, according to [50]. Figure is not to scale.

2.2 Traffic vibrations

Traffic may generate vibrations that can be hazardous for the strength development of young and hardening concrete, and reduce the final bond of new concrete to existing concrete and reinforcement. The greatest concern is when repairs and rebuilding, e.g., bridge deck widening, is carried out while traffic is allowed to pass close to the construction site in adjacent lanes. Several researchers see e.g. [63, 66 and 95], have found that vibrations caused by normal bridge traffic have no detrimental effect on the concrete. None of these researchers

identified any damage from traffic vibration, but nevertheless there are often concerns about permitting traffic on bridge decks during concrete-placing operations. An effective way to reduce the amplitude of traffic-induced vibrations is to maintain a smooth bridge deck surface and to avoid sharp approaches that could lead to impacts from heavy vehicles, [4]. In guidelines and technical specifications a maximum allowed traffic velocity to be often given, e.g. in Norway 40 km/h has been set as a limit while Swedish guidelines used to restrict the velocity of heavier vehicles to 15 km/h, see [7 and Paper I]. The latter also restricted the vibration velocities to a maximum of 30 mm/s, [23], which could be compared with the much higher maximum vibration levels indicated in Figure 2.4. Thus, although the vibration levels generated may be high in some cases the restrictions assigned make traffic-induced vibration harmless to hardening concrete. However, a reduction in the bond to the reinforcing steel may occur in cases with large relative displacements between new and old concrete sections, which should be investigated through structural dynamic analyses. If old and early age concrete sections with its formwork are in synchronous movement the entire structure vibrates as a rigid body, and there will be little risk for damage due to traffic-induced vibrations. Therefore, as commented in [Paper I], due to the low level of PPV, the relatively long duration of vibration and the need for structural dynamic analysis, traffic vibrations are not classified here as impact vibrations and therefore not accounted for in the numerical analyses.

2.3 Machine vibrations and pile-driving

Operating machines and impacts from pile driving generate vibrations with PPV similar to those of traffic but with slightly higher frequencies, as shown in Figure 2.4. There are few investigations of the effects from vibrating machines but some are referred to in [Paper I]. Machines that generate heavy vibrations can be movable machines such as vibratory roller compactors but also static equipment, e.g. ball mills, crushers, pulverizers, compressors, forge presses, see also [64]. It has been observed that construction operating equipment and heavy operating machinery at building sites usually produce vibration velocities below 50 mm/s, which is in the lower range of what is indicated in Figure 2.4. An interesting study is presented by Krell [72]. Tests were done at a coal mill with equipment for pulverization of coal at a power plant. The machinery generated PPV levels up to 80 mm/s within the frequency range 0-200 Hz. The vibrations of the concrete foundation of the mill were recorded and maximum amplitudes were found for the frequency 46 Hz, which is in good agreement with the interval for machine vibrations in Figure 2.4.

Pile driving causes impact-type vibrations that propagate through the ground. However, the distance to newly cast concrete must be relatively short for damage to occur. As an example [121], with normal ground conditions and at a distance of 3 m standard pile driving will not often exceed 50 mm/s. This will only be critical for recently cast very young concrete, e.g. in foundations and slabs in direct proximity to the piling operations. However, strict vibration criteria are often used to obtain a safety factor for the operations and e.g. Siwula et al. [121] recommend that the pile driving activities within a radius of 3 m should not be carried out during the first 5 days after casting of normal concrete and earliest after 1 day for high early strength concrete. Low vibration levels are also reported by Bastian [17], who observed PPV levels around 10 mm/s around concrete close to piling operations. Further in situ tests with young concrete close to pile driving are summarized by Akins and Dixon [3] and Dowding [36].

2.4 Blasting

Construction blasting in hard ground or rock results in stress waves that propagate outwards from the detonation centre, as stress waves that transports energy through the material. During their passage the particles within the material translates and returns to equilibrium, a motion that can be described as displacements, velocities or accelerations. When a wave front reflects at a free surface the particle velocities are doubled and a compressive wave reflects backwards as a tensile wave, etc. The velocity of propagation through elastic materials depends on the type of wave, the most important being longitudinal waves (P-waves) shear waves (S-waves) and Rayleigh waves, see e.g. Dowding [36]. The latter is a surface wave that carries the energy from a blast, or an impact, over long distances while P- and S- waves are more important at close range. Many researchers report blast damage criteria for hard rock and fully hardened concrete, for which the damage levels are often assumed to be close to identical. For Swedish hard rock, Persson [111] reported a PPV of 1000 mm/s as the limit for possible damage, for which Dowding [36] also reported cracking observed in a lined tunnel.

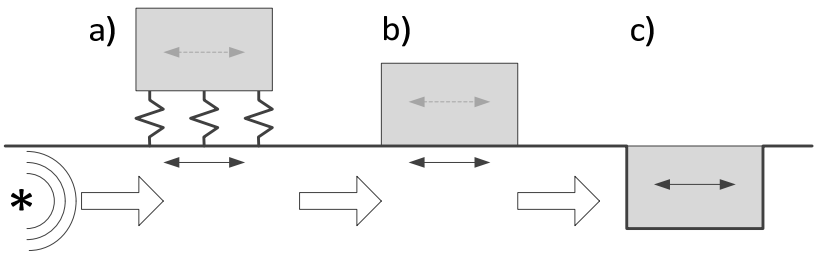

Figure 2.5: Effect from ground impact loads on structural concrete (a), aboveground concrete (b) and underground concrete (c), from [Paper I].

It has been shown that young concrete can withstand fairly high intensity impact vibrations during the first few hours after casting, see e.g. the reviews in [4 and Paper I]. However, the effect of frequency content is important but only addressed by a limited number of researchers, see e.g. [36, 75, 115 and 121]. Of the published safe vibration levels for young concrete close to vibrations that exist, the recommendations by Oriard and Coulson [108] are amongst the very few that also give the dependence of frequency. This is done indirectly by recommending a reduction factor that reduces the limit values when distance from the blast is increased, see [Paper I]. This accounts for the fact that the frequency of motion lessens with distance, which results in increased particle displacement. This attenuation is caused by geometrical spreading and damping in rock or hard ground, [36]. When studying the effect of high intensity impact vibrations such as underground blasting, the type of concrete construction must also be considered. A classification into structural concrete, aboveground concrete and underground concrete, as shown in Figure 2.5, is suggested in [Paper I]. The major difference is here that un-restrained, aboveground structures are free to vibrate and respond as during an earthquake, while restrained, underground structures are forced to deform with the surrounding soil. In the latter case, propagating stress waves from e.g. an underground blasting will directly reach the concrete volume.

Chapter 3

Impact vibration limits and guidelines

Important vibration criteria and published guidelines are evaluated and assessed in [Paper I-VI] within this project. The most important of these are summarized here to provide guidance on what might be appropriate choices for practical use. Based on the state-of-the art report in [Paper I], a summary of vibration criteria for young and hardening concrete and shotcrete subjected to vibration from impact-type loads and blasting is given in the first. These criteria are published by national standards institutes or organizations. Then follows a section that comments on the recommendations and guidelines given in [Paper I and VI], for young concrete subjected to impact-type load. Recommendations for shotcrete, young and also fully hardened, are given in the last section. The latter are based on analytical modelling [Paper III], laboratory testing [Paper II] and finite element modelling [Paper IV-V], and also compared with previous results from [2].

3.1 Standards and specifications

Previous research objectives have included determining threshold levels for human perception of vibrations, as well as preventing and assessing damage to structures and buildings. The effects of vibrations on young and curing concrete have been addressed by relatively few, and a large variation in research recommendations are found due to the absence of in-depth understanding of exactly how the vibration would cause damage to e.g. curing concrete. For curing concrete, vibration limits are prescribed in some codes, standards and specifications or as recommendations compiled by researchers and practicing engineers. A summary of such general national standards that include the vibration close to young and hardening concrete is presented in Table 3.1. More detailed recommendations with respect to young concrete can be found in [Paper I] where it is also concluded that recommendations in national standards and specifications often are conservative, giving values that often are 10 times below what can be observed in situ or in laboratory environments.

In tunnelling, the use of shotcrete is often restricted near the area where blasting takes place, due to the risk of damaging recently applied shotcrete. There are no limit levels for blasting-induced vibrations given in the standards but only recommendations on e.g. minimum compressive strength of concrete or shotcrete. For example, it has been prescribed that the compressive strength should be at least 6 MPa [132] or that the concrete must have reached a strength level of around 60% of the final compressive strength [55] in order to withstand nearby blasting. As a complement to the latter requirement, it is also recommended that the

maximum PPV must not exceed 10 mm/s for shotcrete up to 3 days old. For shotcrete 3–7 days old, the limit is 35 mm/s, and 110 mm/s for shotcrete older than 7 days.

Table 3.1: A comparison of some national standards and specifications for vibrations close to young and hardening concrete, from [Paper I].

Concrete age:	0–3 days	3–7 days	7–28 days	>28 days	Comments:
USA	-	6 mm/s	51 mm/s	-	
China	15–20 mm/s	30–40 mm/s	70–80 mm/s	-	≤10 Hz
	20–25 mm/s	40–50 mm/s	80–100 mm/s	-	10–50 Hz
	25–30 mm/s	50–70 mm/s	100–120 mm/s	-	≥50 Hz
Norway	5–50 mm/s	50 mm/s	70 mm/s	100 mm/s	
Finland	45 mm/s	50 mm/s	70 mm/s	70 mm/s	Distance 1 m
	90 mm/s	100 mm/s	140 mm/s	140 mm/s	Distance 10 m
Sweden	-	-	-	70 mm/s	Distance 1 m
	-	-	-	134 mm/s	Distance 10 m
	30 mm/s	30 mm/s	-	-	If $f_c \leq 12$ MPa

3.2 Young concrete vibration limits

The traditional opinion has been that blasting vibrations up to e.g. 50 mm/s is no threat to early age curing concrete. However, a considerable amount of research has been done to investigate how vibration effects from single events such as a dynamite blast close to young concrete affects its material properties and performance when fully hardened, see e.g. [76]. The published studies and observations have often been carried out under different conditions that make comparison difficult. However, based on the literature survey in [Paper I] the recommended limits shown in Figure 3.1 are selected as representative for young concrete subjected to impact-type vibrations. For a time span of up to seven days, the recommended vibration criteria are given as maximum allowed PPV. On basis of Figure 3.1, recommended maximum vibration velocities are given in Table 3.2, valid for normal strength concrete, cured at +20ºC and subjected to short duration impact-type vibrations at close range, also with recommended limits for corresponding continuous vibrations. Detailed recommendations based on finite element modelling are presented in Table 3.3, with respect to very young concrete, i.e. concrete younger than 12 hours. Recommended damage limits at concrete ages of 4, 6, 8 and 12 hours are given, based on calculations for concrete strength classes C25 and C50, as described in [Paper VI].

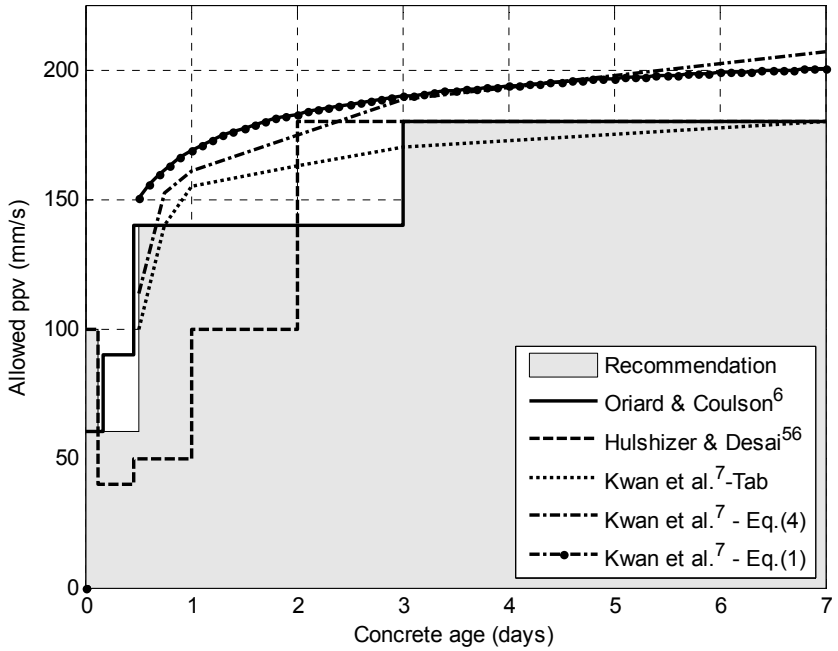

Figure 3.1: Comparison of recommended maximum PPV as function of age for young and hardening concrete. The recommended values from Table 3-2 are shown as a shaded area according to [Paper I].

Table 3.2: Recommended PPV for young concrete in mm/s, from [Paper I]. The limits for continuous vibrations are according to [63].

Vibration type	Concrete age					
	0–3 hours	3–12 hours	12 hours–1 day	1–2 days	2–3 days	3–7 days
Impact	100	60	140	140	140	180
Continuous	(100)	40	40	100	(140)	(180)

Table 3.3: Recommended PPV damage limits for early age concrete, from finite element calculations presented in [Paper VI].

Concrete age, hours	Concrete class C25		Concrete class C50	
	PPV lower limits, mm/s	PPV upper limits, mm/s	PPV lower limits, mm/s	PPV upper limits, mm/s
4	< 30	†	30	†
6	40	†	50	90
8	50	80	70	100
12	60	110	100	200

† Not possible to obtain upper limits

3.3 Shotcrete vibration limits

The performance of young and hardened shotcrete exposed to high magnitudes of vibration is investigated in [Paper II-V]. Safe distances and shotcrete ages for underground and tunnelling construction is discussed, using numerical analyses and comparison with measurements and observations summarized in [5 and 2]. Examples of preliminary recommendations for practical use are given in [2] and it is demonstrated how the developed models and suggested analytical technique can be used to obtain further detailed limit values.

For fully hardened shotcrete, the three analytical models presented in [Paper III] are used for calculations of examples for three different shotcrete thicknesses; 100, 50 and 25 mm. The recommendations for minimum safe distances to a point of detonation of Q = 2 kg of explosives are given in Table 3.4. The results are calculated for two different incoming stress waves with f = 2000 Hz and f = 1265 Hz and with propagation velocities through the rock equal to c = 4000 m/s and c = 2530 m/s, corresponding to E = 40 GPa and E = 16 GPa for the rock, giving the results shown in Figure 3.2. Table 3.4 thus gives a comparison between values for varying rock quality and load frequencies. To represent the occurrence of cracks and imperfections of rock a lower value of the modulus of elasticity is considered, thus the safe distances for f = 1265 Hz are lower than for f = 2000 Hz. The results from [10] are also given for comparison. Note that an increase in load frequency leads to higher load levels and longer safe distances.

The results presented in [Paper IV-V] are used as a basis for recommendation of minimum ages of shotcrete at the time of blasting, exemplified with the recommendations for 100 mm thick shotcrete that are compiled and presented in Table 3.5. Three different shotcrete types are included in Table 3.5, with their development of bond and tensile strength shown in Figure 3.3. The results from [8] are given for comparison as representative for slow hardening shotcrete with waterglass (Sodium silicate) and low temperature curing. It is recommended [Paper II] that the maximum allowable PPVs at the interface between shotcrete and rock are 250 and 500 mm/s within 0–1 day and >1 day, respectively. The results in Table 3.5 are calculated for detonations of 0.5, 1.0, 2.0 and 3.0 kg of explosive at 2.2, 3.0 and 5.0 m from shotcrete on a granite rock surface. The results are obtained from comparison with the bond and tensile strengths given in Figure 3.3, see [Paper V].

Table 3.4: Recommended minimum safe distance for fully hardened shotcrete and detonation of Q = 2 kg explosives, from [2].

Rock and load characteristics	Shotcrete thickness		
	100 mm	50 mm	25 mm
E_{rock}= 16 GPa and f = 1265 Hz	1.8 m	1.0 m	0.7 m
E_{rock}= 40 GPa and f = 2000 Hz	2.5 m	1.5 m	0.8 m
E_{rock}= 40 GPa and f = 2500 Hz [10]	3.5 m	1.9 m	1.2 m

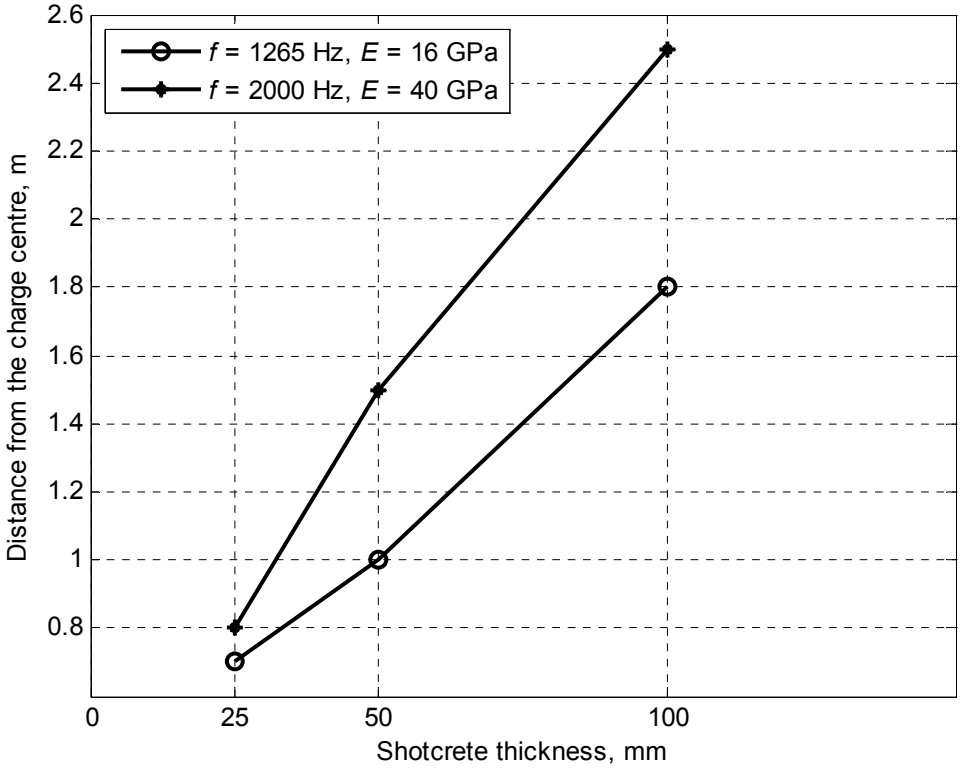

Figure 3.2: Compiled minimum safe distances from detonation of Q= 2 kg. Dependence of load frequency f and rock modulus of elasticity E, [2].

Table 3.5: Recommended minimum ages in hours for 100 mm thick shotcrete of three types. The strength development is shown in Figure 3.3.

	Distance form explosive									
	2.2 m			3.0 m				5.0 m		
Explosives:	0.5kg	1.0kg	2.0kg	0.5kg	1.0kg	2.0kg	3.0kg	0.5kg	1.0kg	2.0kg
Ahmed [2]	12	18	*	10	13	21	-	7	9	12
Ansell [8]	>24	>48	*	24	>24	>48	-	9	21	>24
[Paper V]	-	-	-	-	12	15	23	-	-	-

* Not possible to obtain a sufficiently high bond strength. - Data not calculated.

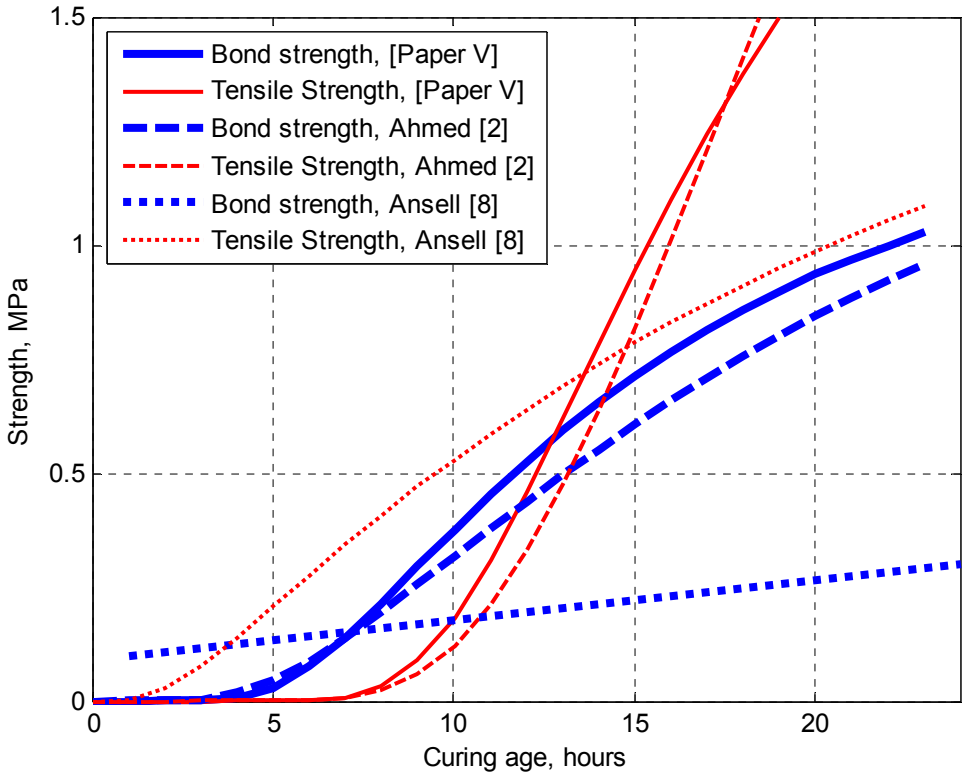

Figure 3.3: Bond and tensile strength vs curing age for the young and hardening shotcrete types referred to in Table 3.5.

Chapter 4

In situ and laboratory investigations

This section describes laboratory tests performed to simulate stress waves travelling through the rock, striking at a shotcrete-rock interface. The tests, thoroughly described in [2] and [Paper II-IV], give data for the investigation and demonstration of how stress waves and structural vibrations are connected. The results are also used for evaluation of the elastic stress wave model, see [Paper III] and Chapter 5, and the bond strength development for shotcrete. In addition, a non-destructive test using the impact resonance method to determine Poisson's ratio at early ages is presented. An earlier laboratory test series and two in situ vibration measurement programs used for comparison and verification of the numerical results presented within the project are also summarized.

4.1 Laboratory testing

4.1.1 Bond failure

An attempt to simulate stress wave propagation through good quality granite, from an explosive charge towards a shotcreted rock surface, has been performed in the laboratory [Paper II]. An experiment was set up with P-wave propagation along a concrete bar, with properties similar to those of hard rock. Cement based mortar with properties that resembles shotcrete was applied on one end of the bar and a hammer impacted the other. For practical reasons, the rock was made of concrete with similar dynamic properties as those of rock and the shotcrete was substituted with cement mortar cast onto one of the quadratic end-surfaces of the concrete bar. The mortar thus formed a slab with the same cross section as the bar, bonding to the end-surface of the bar that corresponds to the rock surface in a tunnel. The layout of a test-bar suspended by cables is shown in Figure 4.1. The concrete beam dimensions and its material properties are given in [Paper II]. A series of tests with 50 and 100 mm thick slabs of shotcrete (mortar) has been carried out where the bar with shotcrete was subjected to different intensity impacts until failure. The tests were performed at shotcrete ages of 6 and 18 hours, as described in Table 4.1, also giving compressive strength of 150 mm cubes, the propagation velocity c, and the bond strength between concrete and shotcrete (mortar). The latter was determined from laboratory pull-out tests where mortar was

cast on concrete plates with pre-drilled ϕ95 mm cores that were pulled out from the bottom of the plates using a testing device able to register the pull-out force [27].

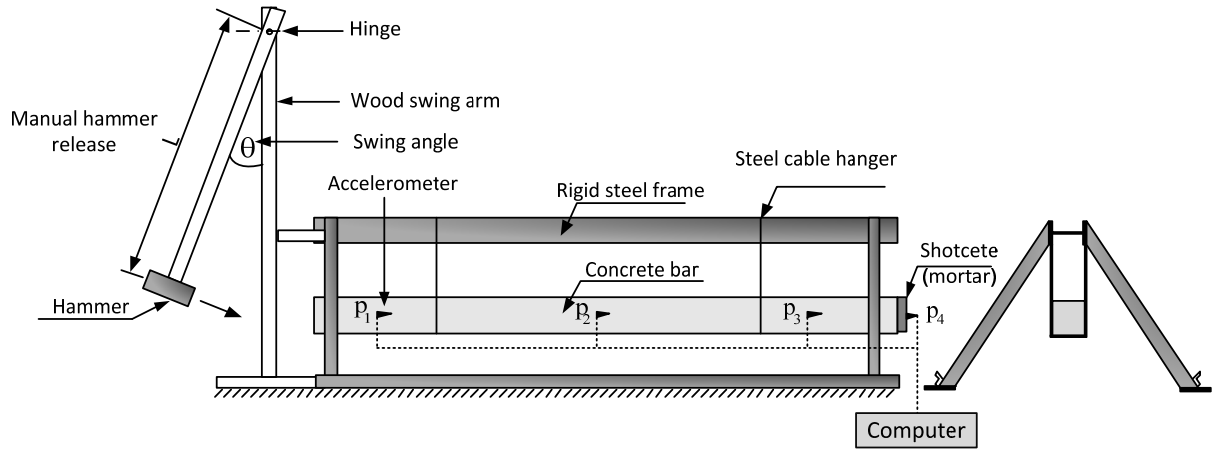

Figure 4.1: Schematic view of the set-up for hammer impact tests, from [Paper II].

Table 4.1: Test series for bond testing, from [Paper II].

Specimen type	Shotcrete thickness, mm	Age, hours	Density, kg/m^3	Compressive strength, MPa	Shotcrete *c*, mm/s	Bond strength [27], MPa
B-S50-6	50	6	2284	0.60	1150	0.1
B-S50-18	50	18	2242	17.0	2266	0.7
B-S100-6	100	6				0.1
B-S100-18	100	18	2268	21.6	2266	0.7

The measurements were divided into two parts; verification of the properties of the test-bar and the search for failure limit PPV for the early age shotcrete. The first part was done to verify that the behaviour of the suspended test-bar is close to that of a free-free bar. Further details are presented in [Paper II]. The acceleration time history and acceleration–frequency spectra for the four points are shown in Figure 4.1, and of specimen B-S100-18 plotted in Figure 4.2. All acceleration time histories and spectra that can be drawn from the performed measurements are similar to these figures. The results from the measured acceleration show two waves that propagate in opposite directions in the bar due to wave reflections, i.e. the incident wave and the reflected wave overlaps. Thus, the acceleration at the middle point (p_2) is the sum of the two opposing waves. When a propagating wave reaches the interface between shotcrete and rock, a part of the wave energy will be transmitted into the shotcrete while the other part reflects back into the rock. This proportion depends on the impedance ratio between rock and the shotcrete, see [Paper II]. The transmitted wave propagates in the shotcrete and reaches the free surface where it is reflected back while doubling the acceleration, see e.g. Dowding [36].

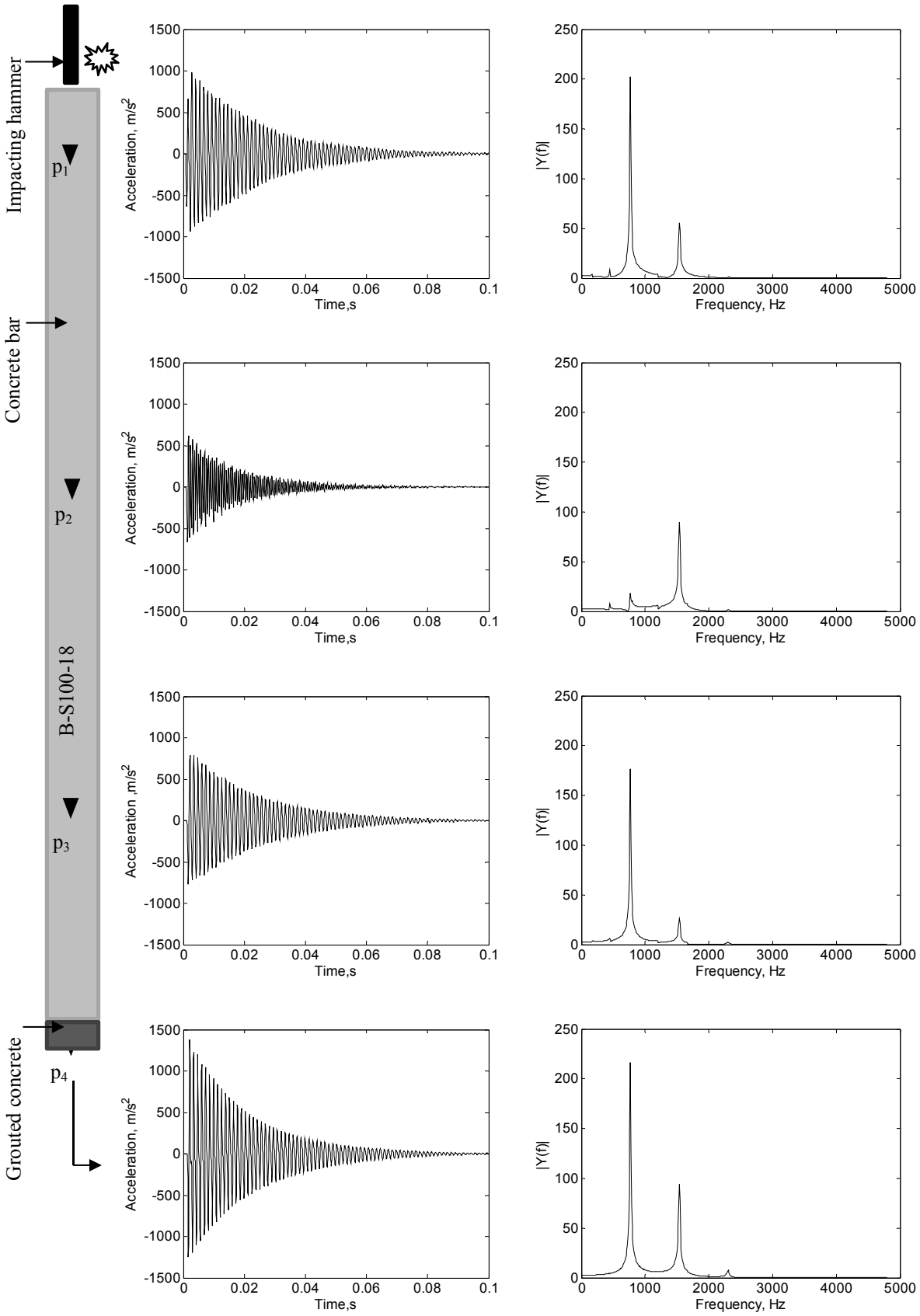

Figure 4.2: Measured acceleration time history and frequency spectra, for an impact velocity of 1.85 m/s, from [2].

It was observed that shotcrete is rigidly tied to the concrete surface until sudden failure occurs. Similar bond behaviour has been observed during testing, [27]. The bond failure was due to the induced stress wave at the opposite end of the bar through the impact of a steel hammer. The tests simulated incoming stress waves, giving rise to inertia forces caused by the accelerations acting on the shotcrete. These will in turn yield stresses at the shotcrete-rock (slab-bar) interface, which may cause bond failure. It is also possible that shotcrete may fail due to low tensile strength, i.e. a failure within the slab.

4.1.2 Poisson's ratio

There are few investigations that present information on Poisson's ratio at early age, and thus it is often reported in the literature that this parameter is insensitive to age, see [105 and 71]. Most published results indicate that the measured Poisson's ratio showed practically the same value for all ages and curing conditions. The majority provides a small number of values for Poisson's ratio at ages from 12 to 30 hours. To date, there is no information given in the Eurocode 2 [40] about how to specify Poisson's ratio at early ages. Although some experimental results [105] show increasing values of Poisson's ratio with age during the first 12 hours, e.g. up to about 25%, this is often considered as an approximately constant value. There are however two important exceptions to this, the studies performed by Byfors [29] and Mesbah [92], who described a significant decrease in Poisson's ratio at very early ages. A decreasing trend of Poisson's ratio from approximately 0.4 to 0.1 during the first 10-15 hours, at a compressive strength of about 1 MPa, [29]. After this, Poisson's ratio increases with strength growth. These observations are also in agreement with the results from an investigation on high performance concrete using the pulse velocity method [92] where Poisson's ratio decreased during a short period of about 9 to 18 hours, reaching a value of 0.14 then increasing to its final values after 7 days. In numerical tests, it was found here that this parameter has a significant effect of the numerical results for early age concrete and therefore, a small scale laboratory test was performed. A non-destructive test was carried out using the impact resonance method where a freely supported (hanging) test specimen is struck with a small impactor and the specimen response is measured using an accelerometer on the specimen. In this test, the longitudinal, transverse and torsional frequencies of the concrete prism at various times after casting were measured so that Poisson's ratio could be calculated, according to testing standard [14]. It should be noted that the same test method was used by Nagy [96], presenting results on which the relation between static and dynamic elastic modulus used in the initial studies [10 and 8] was based. Three accelerometers were positioned on the specimen, as shown in Figure 4.3, enabling the recording of particle accelerations for the three fundamental transverses, longitudinal and torsional resonance frequencies of the concrete specimen. The fundamental frequencies for the three modes of vibration are obtained by proper location of the impact point and the accelerometers, according to [14]. The recording time was approximately 0.03 s with a sampling frequency of 9600 Hz, the highest possible. The recorded signals of impact were low-pass filtered (Bessel filter with 1200 Hz sample rate) before the data was sampled, as described in [Paper II]. The results show similar decreasing trend as in [29 and 92], here shown in Figure 4.4. This figure demonstrates the evolution of Poisson's ratio as function of time for two test prisms. It can be seen that during the first 12 hours, a significant variation of Poisson's ratio occurs, and thereafter stabilizes.

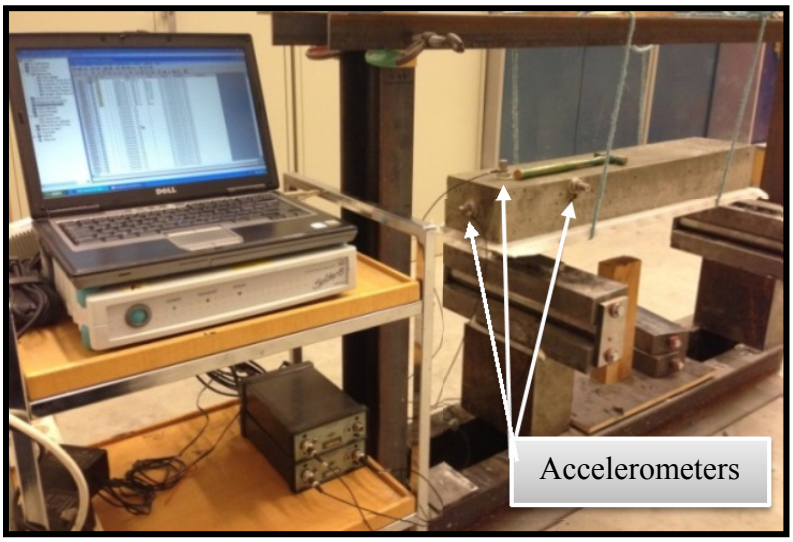

Figure 4.3: The suspended prism and the position of the accelerometers.

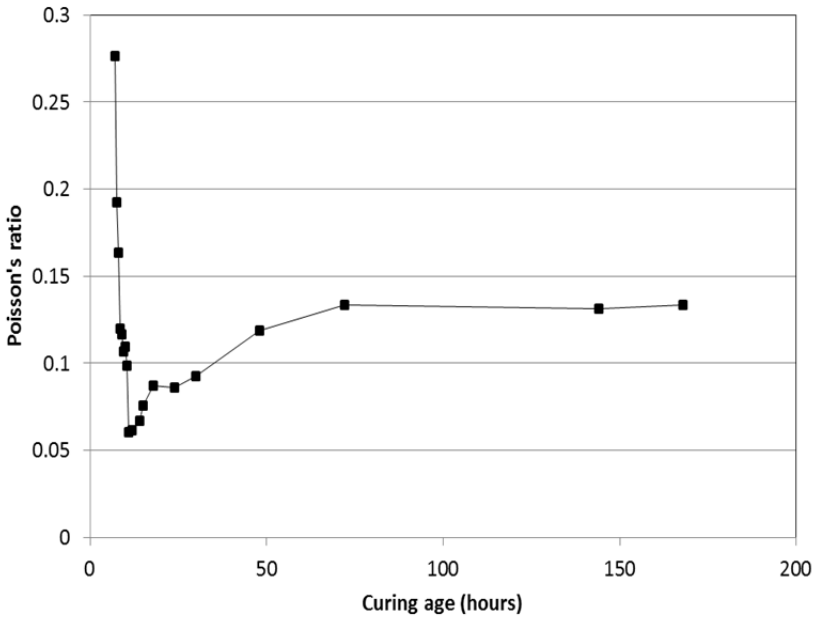

Figure 4.4: Poisson's ratio versus age, example from laboratory testing [Paper VI].

Thus, the variation of Poisson's ratio (v_c) will from now on be assumed to follow the two regression equations given in [29], i.e.:

$$v_c = 0.148\, f_{cc}^{\ -0.486} \qquad f_{cc} < 1 \text{ MPa} \qquad (4.1)$$

and:

$$v_c = 0.128\, f_{cc}^{\ 0.192} \qquad f_{cc} > 1 \text{ MPa} \qquad (4.2)$$

where f_{cc} is the mean compressive cube strength.

4.2 Summary of earlier laboratory tests

For the evaluation of the effect of the shock vibration on young concrete, a limited amount of test results can be found in the literature. This is mainly due to the complexity of performing tests that require the removal of formwork and concrete moulds from early age concrete. For this to be practically feasible, the concrete element must have reached a loadbearing capacity such that it at least can support itself with a certain degree for safety and without excessive deformation or crack formation [116]. In most tests, the concrete specimens e.g. cubes and cylinders, in moulds are mounted on a spring-supported table that was either vibrated or subjected to hammer blows at certain intervals. For long duration vibration tests, shaker tables are often used which provide relatively low levels of PPV, see e.g. [Paper I and 44]. In this type of test the vibration is applied in such a way that the specimens are vibrated as rigid bodies. Laboratory tests that simulate impact loading and stress wave propagation through young concrete have been performed by e.g. Esteves [41], Kwan et al. [75-76] and Gao et al. [47]. In all three of these test series, pendulum hammer impacting is used for the load application. The first attempt to produce impact vibration waves through test specimens was made by Esteves [41], who applied the hammer blows directly to one end of concrete prisms. The vibration tests were conducted at concrete ages of 5 to 20 hours. These tests were performed with the concrete contained in moulds during hammering, whereas Kwan et al. [75] de-moulded the specimens before hammering. For the later tests, the setup is shown schematically in Figure 4.3, where it can be seen that the test specimen are prisms whereas the most common shapes of specimen are otherwise cylindrical or cubic. The concrete prisms with a cross-section of 100×100 mm and a length of 500 mm were subjected to shock vibrations with varying intensity, up to PPV levels of 1200 mm/s.

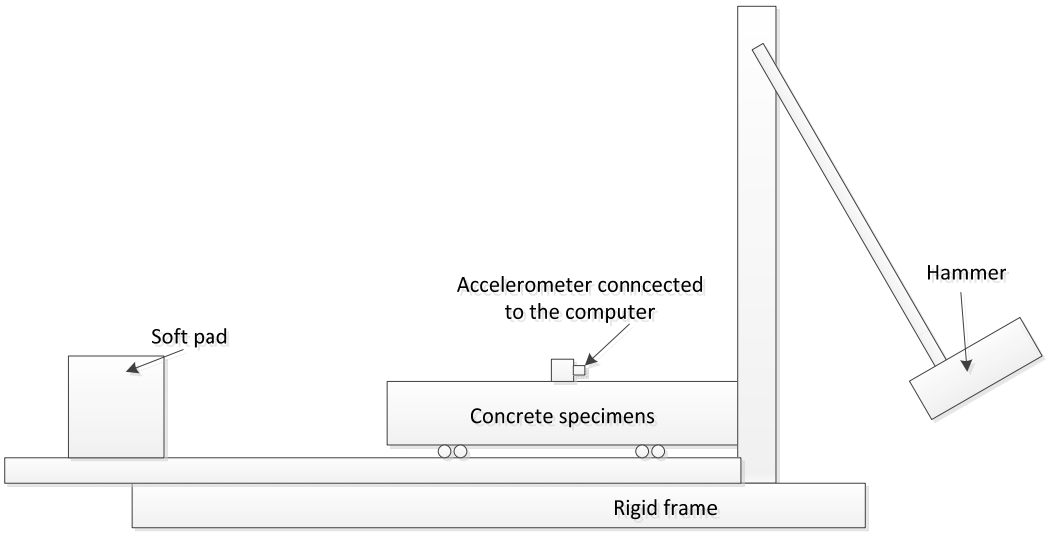

Figure 4.5: Schematic diagram of setup for shock vibration test, from [Paper V].

Before the shock vibration tests, the tested concrete prisms and control specimens were tested for ultrasonic pulse velocities. Thereafter, the prisms were subjected to impacts by applying one hammer blow to each concrete prism, followed by inspection to detect possible cracks and repeated ultrasonic pulse velocity measurements. Upon completion, all concrete prisms were continually cured in a water tank with their longitudinal axes in a vertical direction so that any transverse cracks were kept closed during curing. At the age of 28 days, all the concrete prisms were tested for direct tensile strength in the longitudinal direction and

equivalent cube compressive strength in the transverse direction. An understanding study on the short and long-term effect from impact vibrations is also presented by the same authors [76]. It included the determination of vibration resistance of concrete at different ages, i.e. 12 hours, 18 hours, 1 day, 3 days, 7 days and 28 days, and the recommendation of a new set of vibration control limits, see [Paper I].

A pendulum hammer was also used by Gao et al. [47], with the aim of studying the effect from blasting works on the strength of young concrete. After 1, 2, 3, 5, 7 and 10 days of curing the 100 mm concrete cubes were hammer impacted, resulting in accelerations up to 260 m/s^2. The measured 8-day and 28-day compressive strengths were approximately 41 and 43 MPa.

4.3 Mining blasting measurements

As a first step towards an understanding of the vibration resistance of young shotcrete, in situ tests were conducted in a Swedish mine, [9]. The tests were conducted with sections of plain, un-reinforced shotcrete projected on tunnel walls and exposed to vibrations from explosive charges detonated inside the rock, at ages of 1 to 25 hours, as shown in Figure 4.6. The response of the rock was measured with accelerometers mounted on the rock surface and inside the rock. The tests indicated that the major failure mechanism is sudden de-bonding at the rock–shotcrete interface. It was concluded that shotcrete without reinforcement, also as young as a couple of hours, can withstand vibration levels as high as 500−1000 mm/s while section with loss of bond and ejected rock were found for vibration velocities higher than 1000 mm/s. The results also provided information about stress wave propagation in hard rock, and a scaling relation for PPV as function of distance and explosive charge weight. These values should be compared with the observed damage limits for shotcrete on rock, here compiled in Table 4.2. The results have also been used as input data and for verification in analytical and numerical analytical studies during previous projects [8, 10-11], and within the current project, see [2] and [Paper II-IV].

Table 4.2: Vibration velocities PPV when shotcrete damage occurs based on in situ measurements, from [Paper VI].

	PPV at damage, mm/s	Comments:
Kiirunavaara tests [9]	500–1000	Young shotcrete
Japanese tunnelling [97]	700–1450	
Mining, full scale [69]	app. 1000–1800	
Canadian tests [135]	1500–2000	Steel fibre reinforced

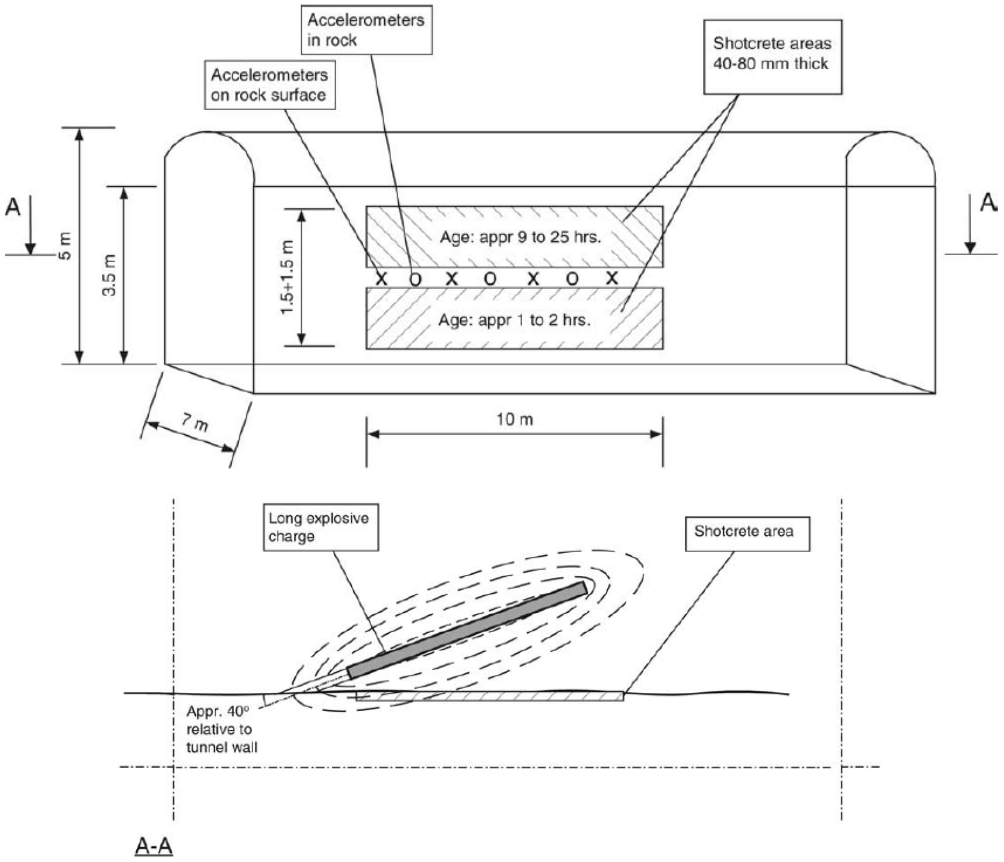

Figure 4.6: Schematic view of a test site. Explosive charge in rock behind shotcrete areas, from [9].

4.4 Tunnelling blasting measurements

Measurements from blasting during the construction of tunnels are presented by Reidarman and Nyberg, [113]. The investigation was performed during construction of the Southern Link (Södra länken) road tunnel system in Stockholm, Sweden, and comprised visual inspection of the shotcrete lining in order to detect cracks and damages. The measurement of vibrations from four blasting rounds was performed using accelerometers located along an axis stretching approximately 5-50 m behind the tunnel front. Accelerations in two directions, parallel with and perpendicular to the tunnel walls, were recorded and later numerically recalculated into corresponding velocity-time records. All measurement points were situated 300 mm into the rock. The layout of the test tunnel with the positions of the measurement points is shown in Figure 4.7. It should be noted that the advancement of the tunnel front is towards the left in the figure and that each blasting round result in 5 m of new tunnel length, except for the third round which gave a 10 m extension. The figure also shows how some measurement points were abandoned in favour of new points closer to the tunnel face, thus approximately giving equal spacing between the points for each of the four rounds.

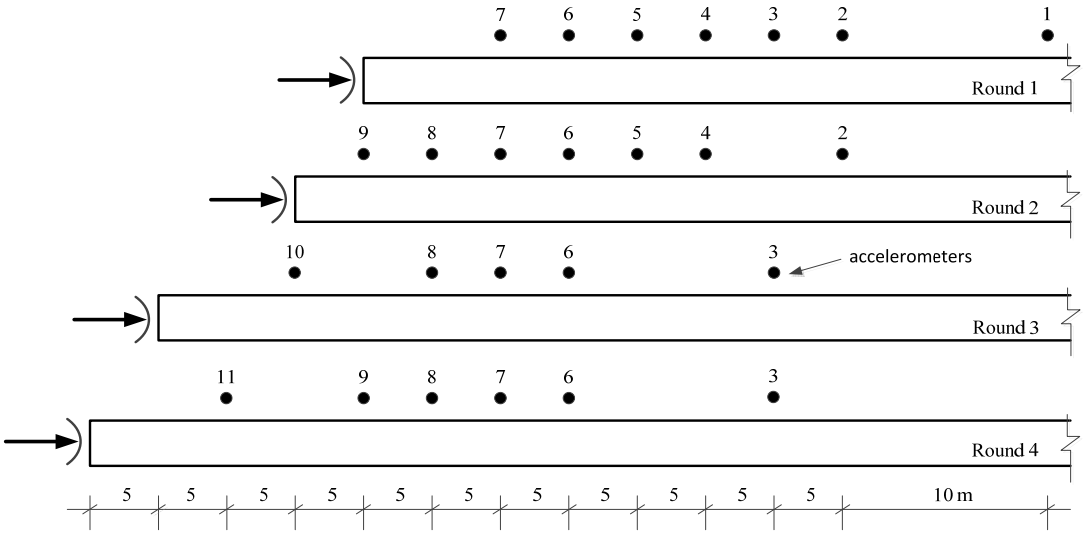

Figure 4.7: Tunnel with advancing front during four excavations rounds. Test layout with positions of measurement points, from [Paper V].

The maximum velocities for each measurement point versus the distances along the tunnel wall are shown in Figure 4.8, where it can be seen that the largest PPV levels were recorded within the nearest 20-30 m to the explosives. The results are here referred to in the study presented in [Paper V], used for comparison and verification of the numerical model that describes impact stress propagating through hard rock, towards recently sprayed concrete linings.

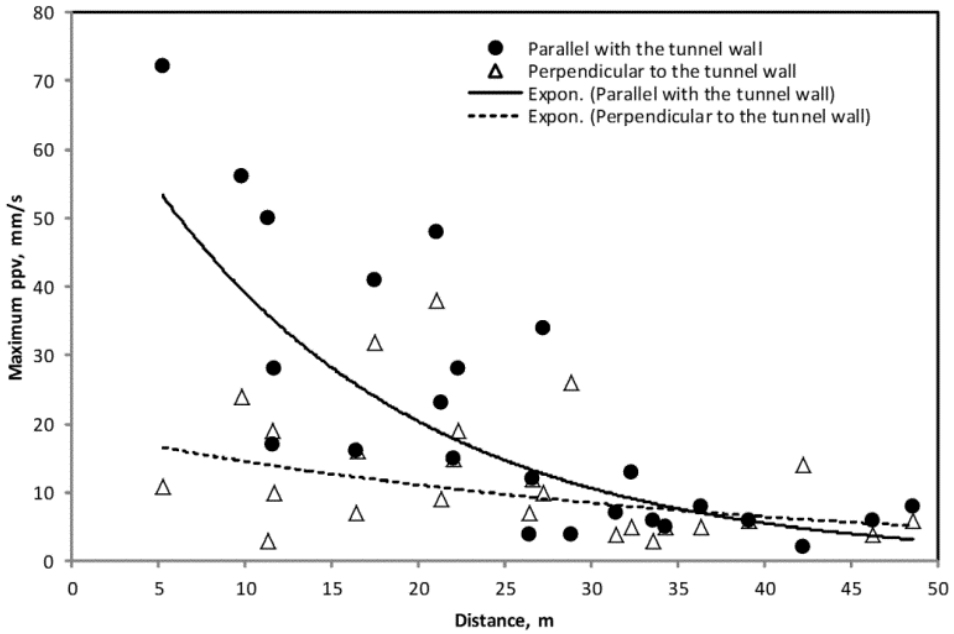

Figure 4.8: Maximum PPV versus distance along the tunnel wall, from [Paper V].

Chapter 5

Dynamic analysis

Shotcrete support in hard rock tunnels is here first studied through numerical dynamic analysis using three different engineering models with elastic material assumptions. In all three models the rock is exposed to P-waves striking perpendicularly to the shotcrete-rock interface. The calculated stress responses in shotcrete closest to the rock surface are then compared. Two-dimensional (plane strain) dynamic finite element models of shotcrete and rock subjected to stress waves are also investigated. These finite element models are also based on elastic material theory and used to simulate the stress waves from blasting, propagating in rock towards shotcrete on a tunnel wall. As a further development, three-dimensional finite element model based on non-linear material formulations is used for modelling smaller scale laboratory tests of impact loaded young concrete prisms. This model can also describe cracking within the concrete volumes studied.

5.1 Structural dynamic models

The first of the structural dynamic models consists of lumped masses and spring elements and the second is built up with finite beam elements and connecting springs. The third is a one-dimensional elastic stress wave model. The three models are thoroughly described in [2] and [Paper III] where they are also compared through a series of numerical examples. Cases with detonation of 2 kg of explosives for a distance up to 7 m between shotcrete and centre of the explosives are compared. The maximum interface stresses that build up between shotcrete and rock for thickness of 100, 50 and 25 mm are given. For the stress wave model the dynamic load is defined as a time dependent velocity while a time dependent acceleration is used for the other two model types. The three models are based on linear elastic material theory and thus not able to describe partially damaged structures, e.g. partial de-bonding of shotcrete. As a simple way to identify the limit for damage, series of calculations are performed with increasing the load level until either the tensile strength or the bond strength is exceeded.

By using the theory of structural dynamics in analysing the response of structures to ground acceleration caused by earthquake, the stress wave propagation within the shotcrete layer can be described. The mass-spring system tested is shown schematically in Figure 5.1 and consists of lumped masses connected with elastic springs, i.e. a linear system with damping disregarded. For this linear system, the relationship between spring force and resulting

displacement depends on the stiffness of the system. The acceleration load is applied following the same principles as in an earthquake analysis, here using Duhamel's integral to calculate the response to the ground acceleration. The constitutive material relationship is used to calculate the stresses within the material where the strain is obtained by dividing the deformation by the original length, for a unit area of the shotcrete layer.

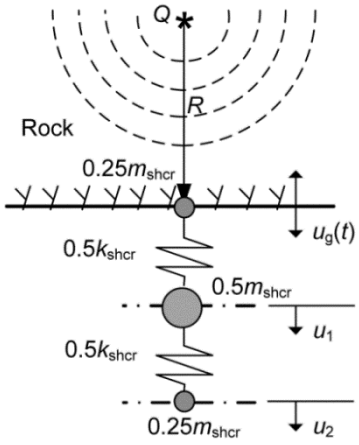

Figure 5.1: Mass-spring model with lumped masses and springs representing shotcrete exposed to vibrations from an explosive charge Q, from [2].

The fundamentals of the beam-spring model are shown in Figure 5.2, where a section of rock with shotcrete is modelled using beam elements that represent flexural stiffness and mass. The beams are attached to the ground with elastic springs that also account for movement parallel to the rock surface. A beam element coupled to elastic springs at each end can be described by adding spring stiffness to the beam element stiffness. The maximum allowed spring elongations to be given by the tensile bending strength of rock and the bond strength between shotcrete and rock. The stresses that appear at the interface between rock and shotcrete are thus proportional to the elongation of the springs. In this two-dimensional model, the load is represented by the time-dependent accelerations and the resulting response obtained through mode superposition analysis.

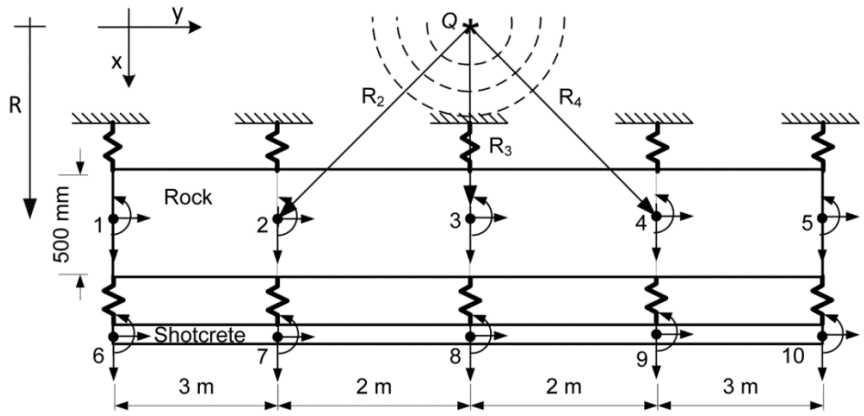

Figure 5.2: Beam-spring model of shotcrete and rock exposed to vibrations from an explosive charge Q. Beam and spring elements interconnected at nodes with three degrees of freedom, from [2].

The stress wave model is based on the theory of elastic waves, describing one-dimensional, longitudinal P-wave (first arriving wave) propagation. The transmitted and reflected waves are superposed to calculate the total stress in the shotcrete layer. A graphical description of the model is given in Figure 5.3 where a shotcrete strip with unity cross-section area is divided into multiple elements. The shotcrete-air interface is defined as a boundary condition and the thickness of each element, Δx, is chosen so that in each time increment of the analysis the wave has propagated a distance of one element.

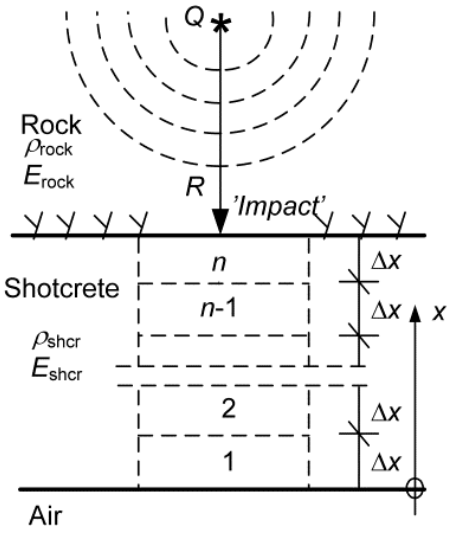

Figure 5.3: Elastic stress wave model of a shotcrete lining on a rock surface, exposed to a stress wave from an explosive charge Q, from [2].

Limiting distances for safe blasting can be estimated by plotting series of maximum stresses, obtained from results of these three models, versus the distance from the explosive charge. An example of this is shown in Figure 5.4, where series calculated with the three models are compared. The results are valid for 25 mm and 100 mm thick shotcrete and with a constant weight of explosives that is Q = 2 kg. The maximum bond stresses that are developed between shotcrete and rock as a function of the distance are, in Figure 5.4, shown for one weight of explosives Q.

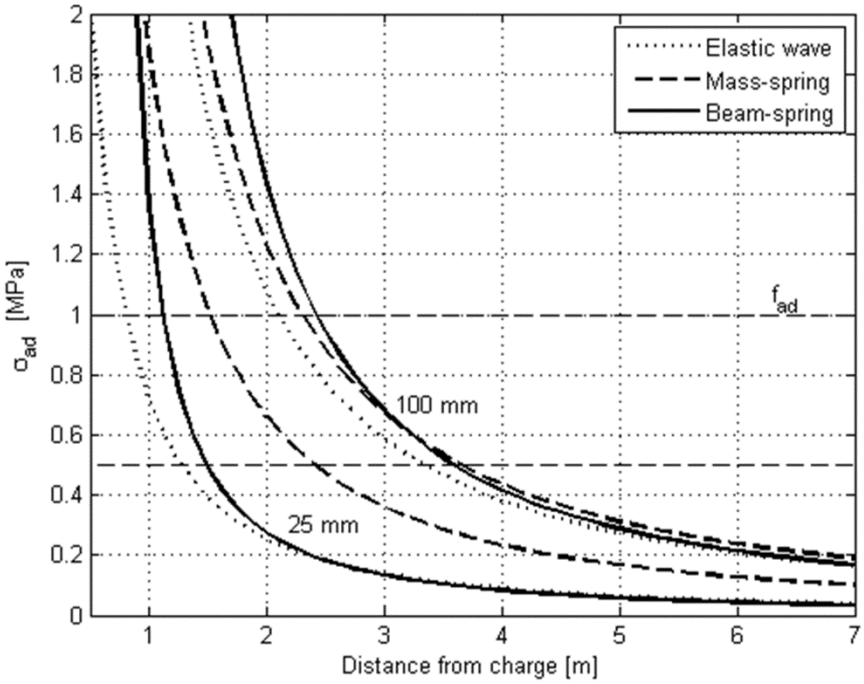

Figure 5.4: Examples of maximum bond stresses between shotcrete and rock versus distance from a 2 kg explosive charge (ANFO). For 25 mm and 100 mm thick shotcrete. The bond strength σ_{ad} is 1 MPa [Paper III].

5.2 Finite element models

5.2.1 Wave propagation in prototype rock

The effect of impact loading and wave propagation has been studied using non-destructive laboratory experiments, as mentioned in Section 4.1. Finite element modelling was used to verify the test results, which showed that the laboratory model with an impacting hammer could produce the same type of stress waves that is the result from blasting in good quality rock. The engineering simulation software Abaqus [120] was used to create a three-dimensional finite element model analysed with the Abaqus/Explicit solver. The model of the test-bar is shown in Figure 5.5, with details on the used solid elements and features presented in [Paper II].

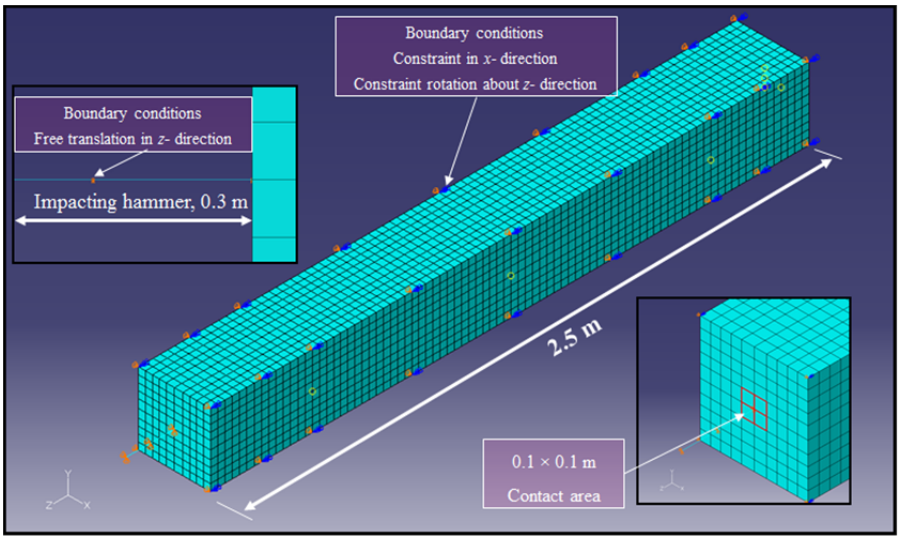

Figure 5.5: Finite element model of the experiment bar, from [Paper II].

Shotcrete was here represented by cement mortar cast onto one of the quadratic end-surfaces of the bar. The mortar thus formed a slab with the same cross-section as the bar, bonding to the end-surface that corresponds to the rock surface in a tunnel. The interaction between the hammer, the concrete bar and the shotcrete layer was constrained using displacement boundary conditions, restricting the model to primarily describe particle displacements in the wave propagation direction. Between the concrete bar and the hammer free translation was allowed in the longitudinal direction only. The shotcrete slab was rigidly tied to the concrete surface to simulate the bond behaviour observed during testing [27], i.e. full contact until a sudden failure. The incident disturbing stress wave, caused by the hammer, was applied as surface-to-surface contact using the kinematic contact method with definition of the initial velocity in the longitudinal direction of the hammer, with the velocity assumed to follow the pendulum equation [Paper II].

5.2.2 Tunnelling blast vibrations

Dynamic finite element models of rock and shotcrete subjected to stress waves have been developed using the Abaqus/Explicit finite element program [Paper IV]. The simulations were performed using two-dimensional (2D) plane strain elements. The models describe two cases with respect to the geometry of the tunnel and position of the detonation point. The fundamentals of the models are shown in Figure 1.1. The detonation is introduced in the model from a circular area within the rock where an impulsive particle velocity is applied. An incident PPV wave caused by an explosion is applied as a boundary condition at the perimeter of the circular area, with the radius R_{PPV} where the particles velocity reaches the threshold PPV = 900 mm/s. This distance corresponds to the limit for rock damage [111] and therefore elastic properties can be assigned to the rock outside this area. In the real case, the rock in close vicinity to the hole containing the explosives will be severely cracked. However, there is no need to include this effect in the present model since the load is applied at a long enough distance from this point.

An example of meshing and use of finite elements is shown in Figure 5.6, to be compared with the left case in Figure 1.1, here with a fine mesh used around the loading area and tunnel

opening with coarser mesh farther away from the tunnel opening. Infinite elements were used to represent the non-reflecting boundaries and prevent the wave reflections. The rock and the shotcrete behave in a strictly elastic manner and possible failure thus occurs when the stresses at the shotcrete-rock interface exceed the bond strength. That is, no plastic deformations or permanent failure, for example crushing or cracking, were considered within the models and a linear elastic relationship between stress and strain was assumed. The horseshoe shaped tunnel with a height of 6 m and width of 5 m is assumed to be situated 11.5 m below the ground surface. The material surrounding the excavation is discretized with first-order 4-node plane strain elements of type (CPE4R), recommended for simulations of impact and blast loading using Abaqus/Explicit [120]. The infinite extent of the rock is represented by a 20 m wide mesh that extends from the surface to a depth of 45 m below the surface. Far-field conditions on the bottom and right-hand side boundaries are modelled using infinite elements of type (CINPE4). The interaction between rock and shotcrete was modelled using tie constraints, i.e. no relative displacement between the materials was assumed. The element size of the shotcrete part is 0.01×0.1 m^2 for all models, with different element sizes used for the rock part. Depending on the accuracy and details of the solution, some regions of the rock would be discretized with a refined mesh. More refinement adjacent to the tunnel opening and loading area was done, due to the significant deformations expected at these regions. The model consists of about 28000 nodes and 25000 elements.

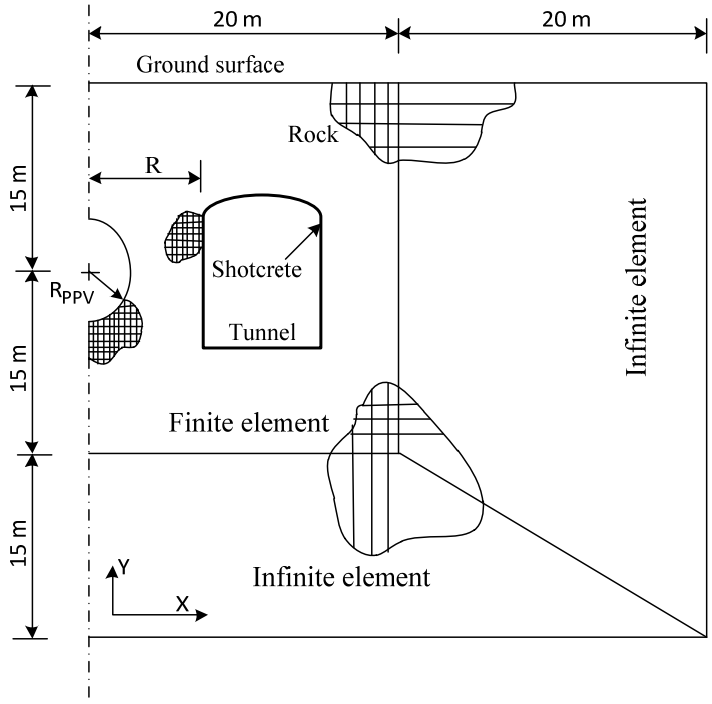

Figure 5.6: Configuration of a finite element model for a tunnel cross-section, from [Paper IV].

By applying a particle velocity at the charge hole as a velocity boundary condition, the propagation of the waves in the rock was investigated. In the examples presented in [Paper IV], a damping ratio of 8% is used, estimated from in situ measurements. The shotcrete was assumed to have a density of 2100 kg/m^3, a modulus of elasticity of 27 GPa and the rock a density of 2500 kg/m^3 and a modulus of elasticity of 40 and 16 GPa for intact and fractured rock, respectively. The detonation of Q = 2 kg of explosives, corresponding to ANFO (ammonium nitrate and fuel oil), is considered for series of calculations for the two

cases in [Paper IV]. The principal frequency of the incident particle velocity is assumed to be 2000 Hz for all models. Results for 100 mm thick shotcrete are studied. In addition, examples demonstrating the effect of shotcrete age are also presented, for detonation of Q equal to 0.5, 1.0 and 2.0 kg, respectively. The dynamic excitation can be described as a cosine-pulse velocity or a corresponding sine-pulse acceleration [2].

Results from a series of models with varying distance between shotcrete and explosive charges are presented in [2]. In addition to the case of the horseshoe shaped tunnel profile presented in [Paper IV], the tunnel plane shown in Figure 1.1 is included in this section (Figures 5.7 – 5.10) to show how the explosion generates stress waves that propagate towards the shotcreted tunnel walls. Due to this motion, the stresses on the shotcrete vary in time, being the sum of the incident and reflected stress waves. The calculations were carried out with R = 3.0 m from the centre of the charge. The same boundary conditions as used in [Paper IV] are assumed. The stresses in the x- and y-directions are presented in Figures 5.7–5.10 and indicated with red areas showing tensile stresses (positive) over 0.2 MPa and blue showing compressive stresses (negative) lower than -0.2 MPa. Far away from the charge hole and the tunnel, zero stress (green) can be assumed.

A feature of finite element stress analysis is the large amount of data generated, making the information suitable for presentation in graphical form. The stress distributions due to blasting loads applied as boundary conditions at the perimeter of the circular area with the radius R_{PPV}, are shown in Figures 5.7–5.10. The stresses that are developed around horseshoe shaped tunnel profiles are depicted in Figures 5.7–5.8. Shortly after the explosion, the compressive stress waves in the x-direction (σ_x) reach the tunnel and are transmitted into the thin layer of the shotcrete tied to the rock surface. Then, the compressive stress waves start to reflect at the surrounding rock, as shown in Figure 5.7. Reflected, tensile stress waves appear on the upper and lower sides of the shotcrete layer continuing towards the end of each side, being concentrated around the corners. In Figure 5.8, the contour of the stresses in the y-direction (σ_y) are depicted. It can be seen that the reflected tensile stresses appeared only on lower sides of the tunnel, see Figure 5.8. It should be pointed out that the time span of the analyses is 10×10^{-3} s and absorbing boundaries were used to eliminate stress wave reflection from the outer edges of the models, beyond which the rock continues.

The models of Figures 5.9–5.10 demonstrate detonation ahead of a tunnel front and the stresses that are developed along the tunnel walls, see [2]. The centre of the explosive charge was here located 3 m from the front. Compared with the results in [Paper IV], this is a safe distance with respect to damage at the front where the vibration velocity is v_{max} = 470 mm/s, as given in [2], i.e. just below the previously defined damage limit of 500 mm/s, [9]. The results in Figure 5.9 show a dominance by stresses along the tunnel walls; i.e. in the z-direction (σ_z). Of the three previously used engineering models in [Paper III], shear stresses only could be described by the beam-spring model. In the study of large scale blasting during mining operations [8] where stress waves reached the shotcrete at an oblique angle, domination of shear stresses was also observed. It can be seen that the only high normal stresses (x-direction) appear locally just behind the tunnel face while the maximum shear stresses (z-direction) are situated 2 m into the tunnel. In addition, note that the shear stresses are present more than 10 m into the tunnel. See [Paper IV], for more details. Figure 5.10 shows that after the explosion the tensile stresses in x-direction (σ_x) appeared on both shotcreted sides of the tunnel.

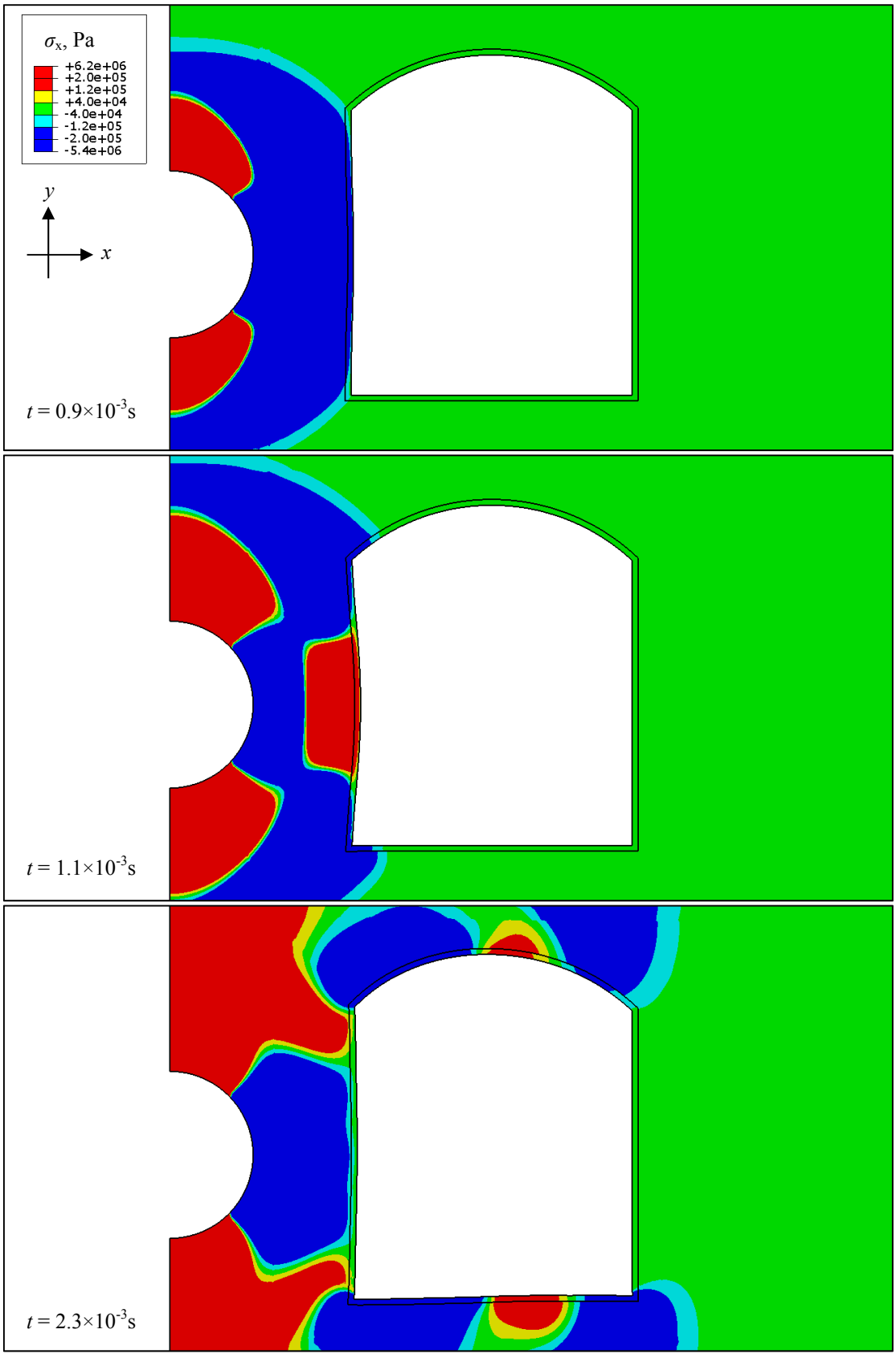

Figure 5.7: Contours of stresses in x-direction (σ_x) of the horseshoe shaped tunnel. Deformation scale 1:1000, from [2].

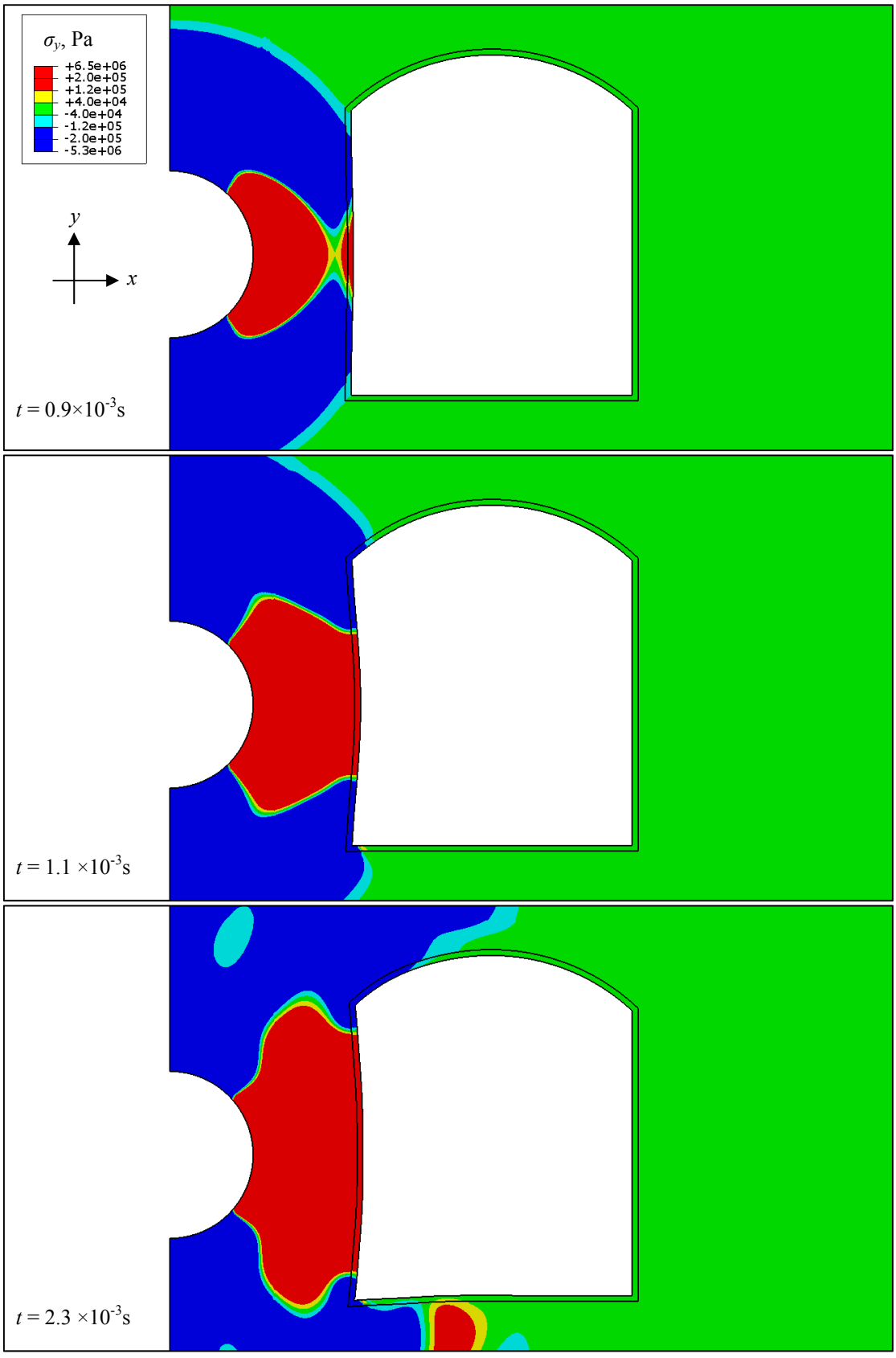

Figure 5.8: Contours of stresses in y-direction (σ_y) of the horseshoe shaped tunnel. Deformation scale 1:1000, from [2].

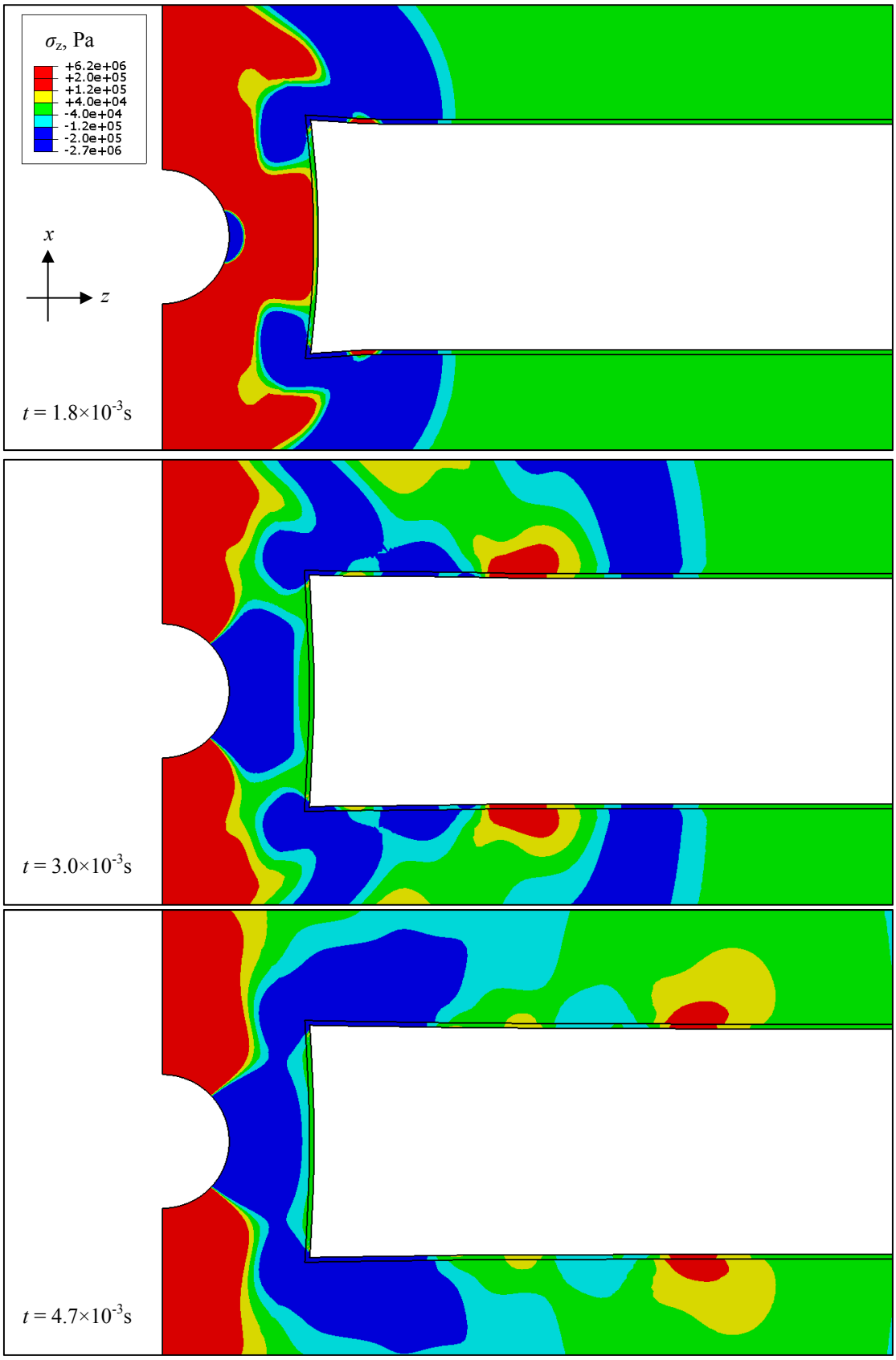

Figure 5.9: Contours of stresses in z-direction (σ_z) of the side walls of the tunnel. Deformation scale 1:1000, from [2].

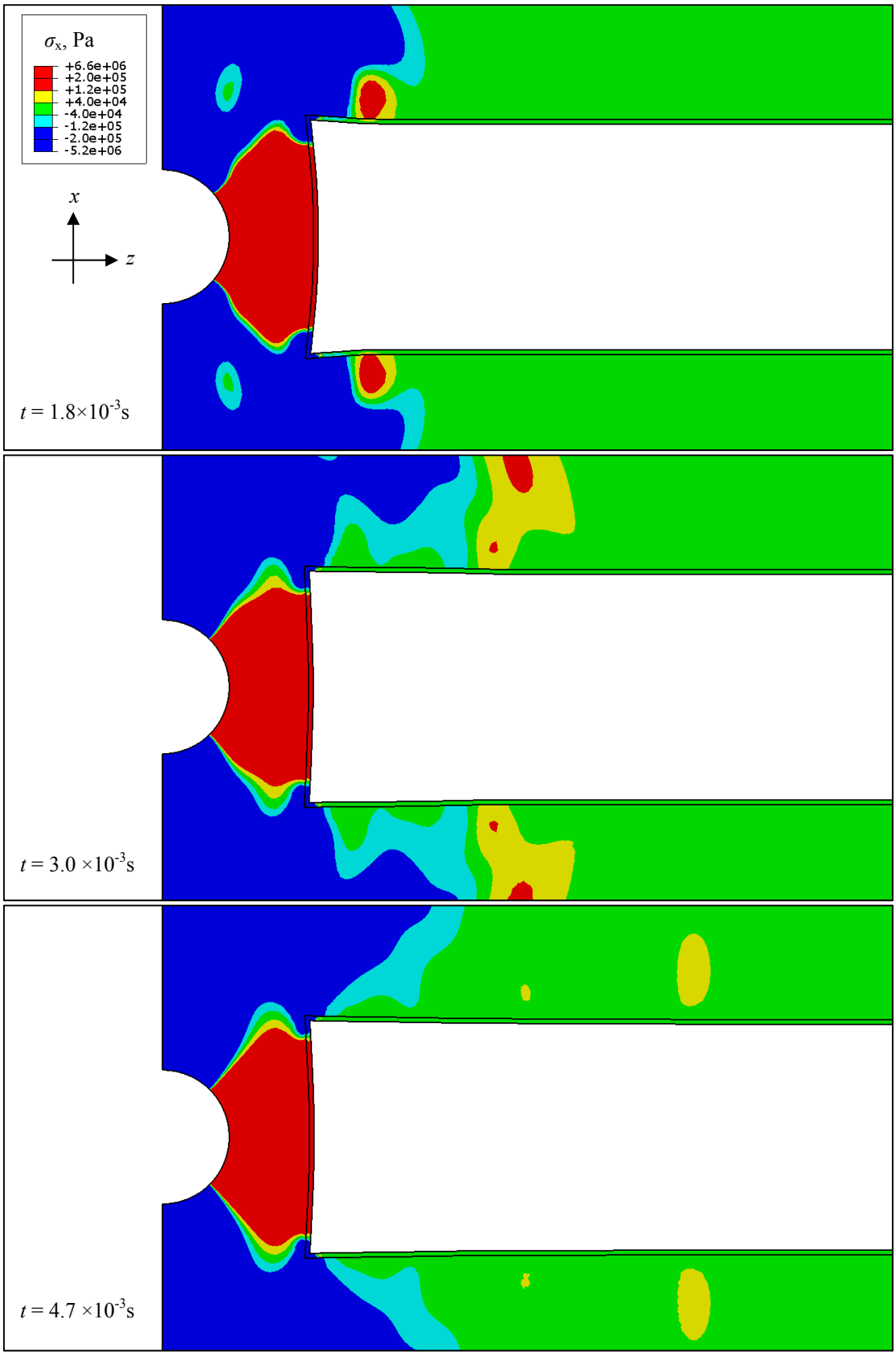

Figure 5.10: Contours of stresses in x-direction (σ_x) of the side walls of the tunnel. Deformation scale 1:1000, from [2].

5.2.3 In situ case study

The results from the in situ investigation presented in Section 4.4 are well suited for evaluation of the finite element models described in the previous section. No shotcrete damage was observed following the blasting, due to the very strict guidelines used, and it can thus be assumed that the shotcrete-rock system behaves elasticity throughout the passage of the stress waves. The finite element model, based on elastic material properties, can therefore be used for a numerical study of the stress wave propagation along these tunnel walls. For this case study, a 2D model of the horizontal tunnel plane is used (see Figure 1.1, right case), since a full 3D model has been much more computationally demanding. The model describes the same deformations as the measurement set up used by [113], with accelerometers positioned on a horizontal line along the tunnel length. The fundamentals of the model where the wave propagates through the rock from the detonation point at the centre of the charge towards the front of the tunnel and along the tunnel sides, as well as an example of meshing and use of finite elements are shown in Figure 5.11. The detonation is introduced in the model from a circular area within the rock where an impulsive particle velocity is applied. The incident PPV wave caused by an explosion is applied as previously described in Section 5.2.2, i.e. as a boundary condition at the perimeter of the circular area with the radius *R*ppv. The model consists of about 27000 nodes and 26000 elements and the analysis example is based on the material properties given in [Paper V], valid for cases with 100 mm shotcrete.

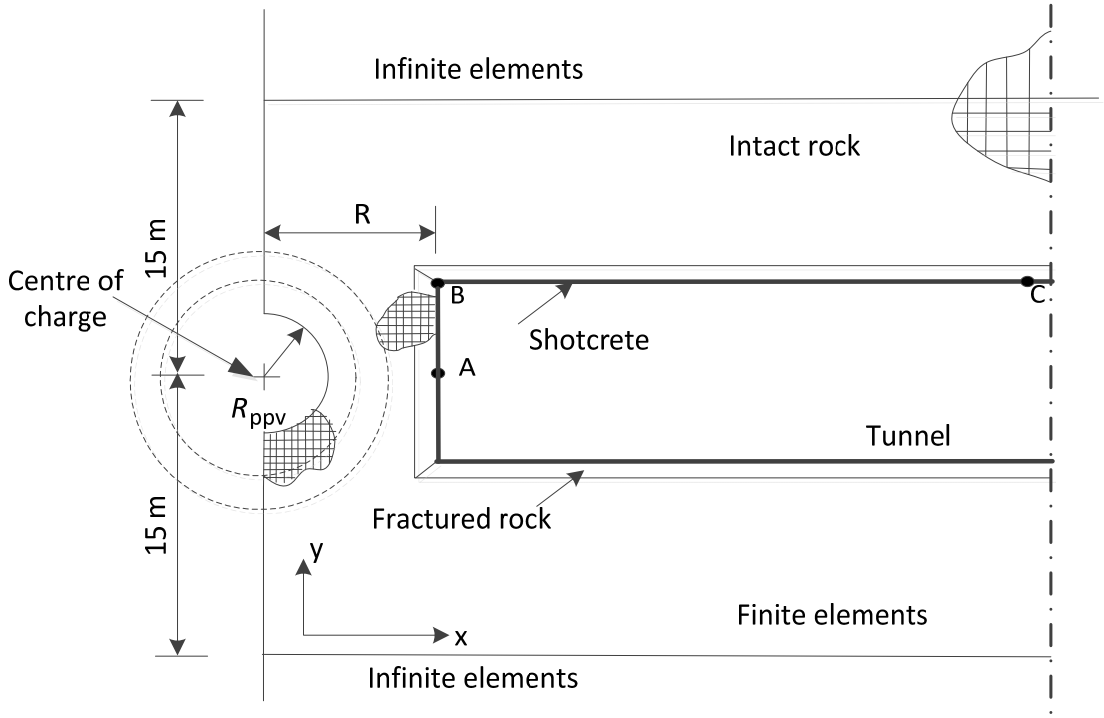

Figure 5.11: The detonation in rock ahead of the tunnel face (horizontal plane). Configuration of finite element model [Paper V].

The response of the shotcrete in the tunnel is investigated for higher blast loads, using 2 and 3 kg of explosives in [Paper V]. Under the higher blast loads, the shotcrete stress along the tunnel length increased, giving stress concentrations of which an example can be seen in Figures 5.12–5.13, where the stress distributions are shown. The stresses in the x- and y-directions are indicated with red areas showing tensile stresses (positive) over 1.0 MPa and

blue showing compressive stresses (negative) lower than -1.0 MPa. Far away from the charge hole and the tunnel, zero stress (green) can be assumed. It can be seen that at 2 ms after the detonation, the first peak of shear stress, see Figure 5.12, is concentrated mainly at the tunnel front while at 2.7 m peaks of high shotcrete stress can be seen forming close to the corners between front and wall, see Figure 5.13. Such stress concentrations also propagated along the tunnel walls, but with decreasing stress levels. It should be pointed out that the analysis covered 100 ms duration.

5.2.4 Mass concrete subjected to impact

For recently placed concrete exposed to impact vibrations, not many attempts have been made to explain the mechanisms behind possible damage and how this change with concrete age. Several investigations focus on identifying the maximum vibration levels that can be accepted and there is published relevant data from measurements conducted during pile driving and blasting, e.g. [61, 63, 75-76 and 121], and from traffic loads during repair, extension or widening work on concrete bridges, see e.g. [54, 88 and 99]. A more detailed summary of relevant literature is given in [Paper I]; from which three major issues can be observed. The first is how a vibration test should be conducted to accurately measure and identify the threshold vibrations that cause damage. Different test methods have been used, leading to widely different results, and up to now there is no mainly acceptable vibration test method. The second issue is what damage types to expect the curing concrete, the most obvious being cracking [88]. There may also be de-bonding of reinforcing bars and other types of strength reduction for the concrete, which are not directly observable. Some researchers rely on visual inspection of surface cracks to detect vibration damage to the concrete. However, according to [1] this approach is not a reliable method for detecting vibration damage because only macro-cracks can be observed with the naked eye. Others evaluate the vibration damage by measuring changes in cylinder compressive strength, split cylinder tensile strength or ultrasonic velocity of test specimens [2], despite that the measured changes in compressive or tensile strengths depend on how these are measured. However, the probable effects of tensile stresses are extension of existing micro-cracks, generation of new micro-cracks and reduction in tensile strength. The third issue is what factors affect the vulnerability of curing concrete to vibrations. It has been suggested that concrete quality, e.g. slump and bleeding, and the reinforcement details, e.g. cover and anchorage, should have some effect on the vulnerability of curing concrete to vibration [7], but exactly how is still not fully understood. However, more research is needed in order to clarify this importance, considering the frequencies of impact induced vibration as well as the intensity of PPVs.

Due to the difficulties in performing experiments on early age concrete, e.g. due to early formwork removal problems, finite elements models, presented in [Paper VI], are used to make it possible to investigate the threshold impact vibration intensity that would cause vibration damage on concrete younger than 12 hours, whenever the model is precise enough to adequately produce impact waves that propagate through the concrete. The model presented here allows for non-linear analysis of concrete, more details presented in [Paper VI].

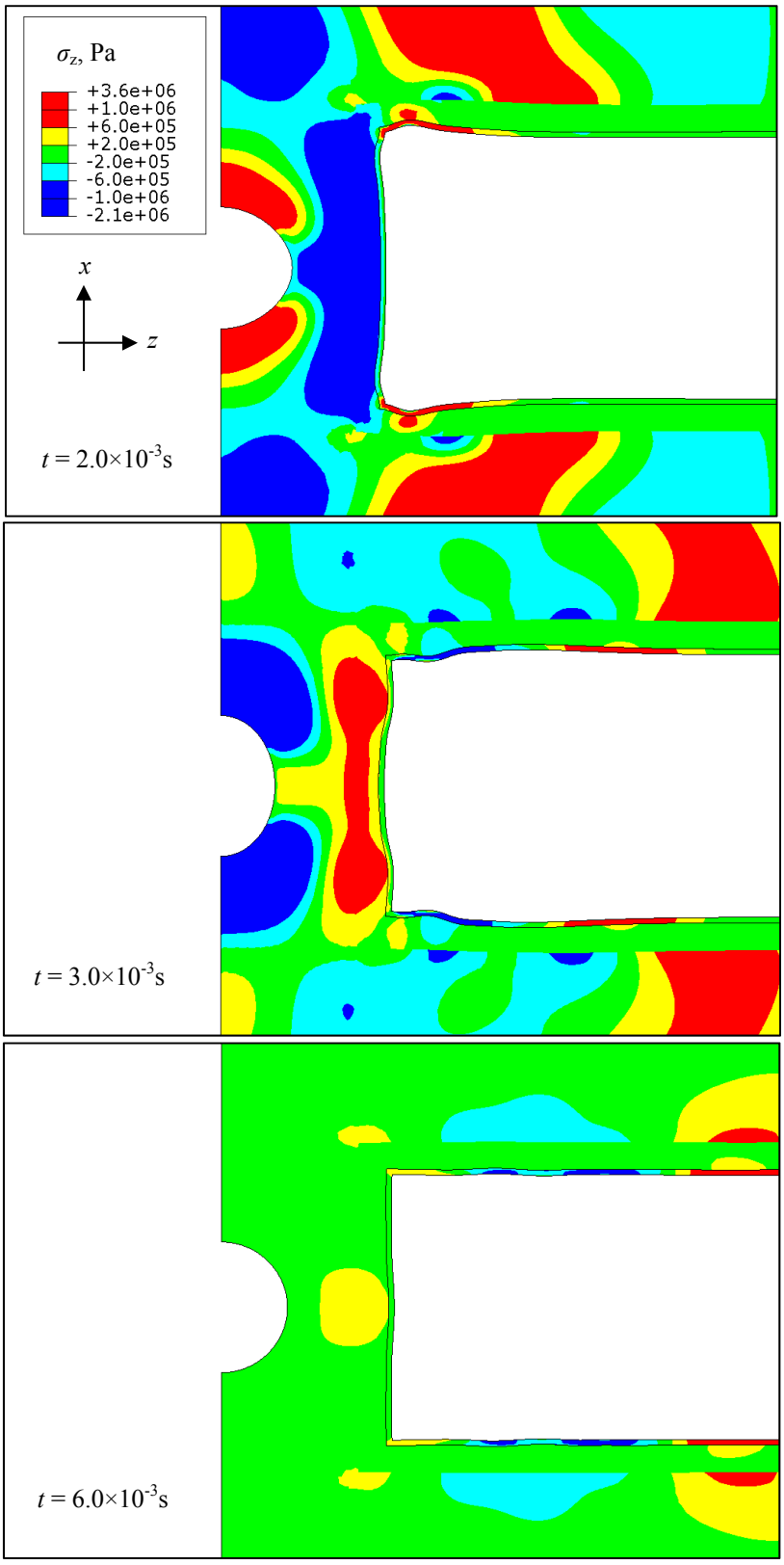

Figure 5.12: Contours of stresses in z-direction (σ_z) of the side walls of the tunnel. Deformation scale 1:1000.

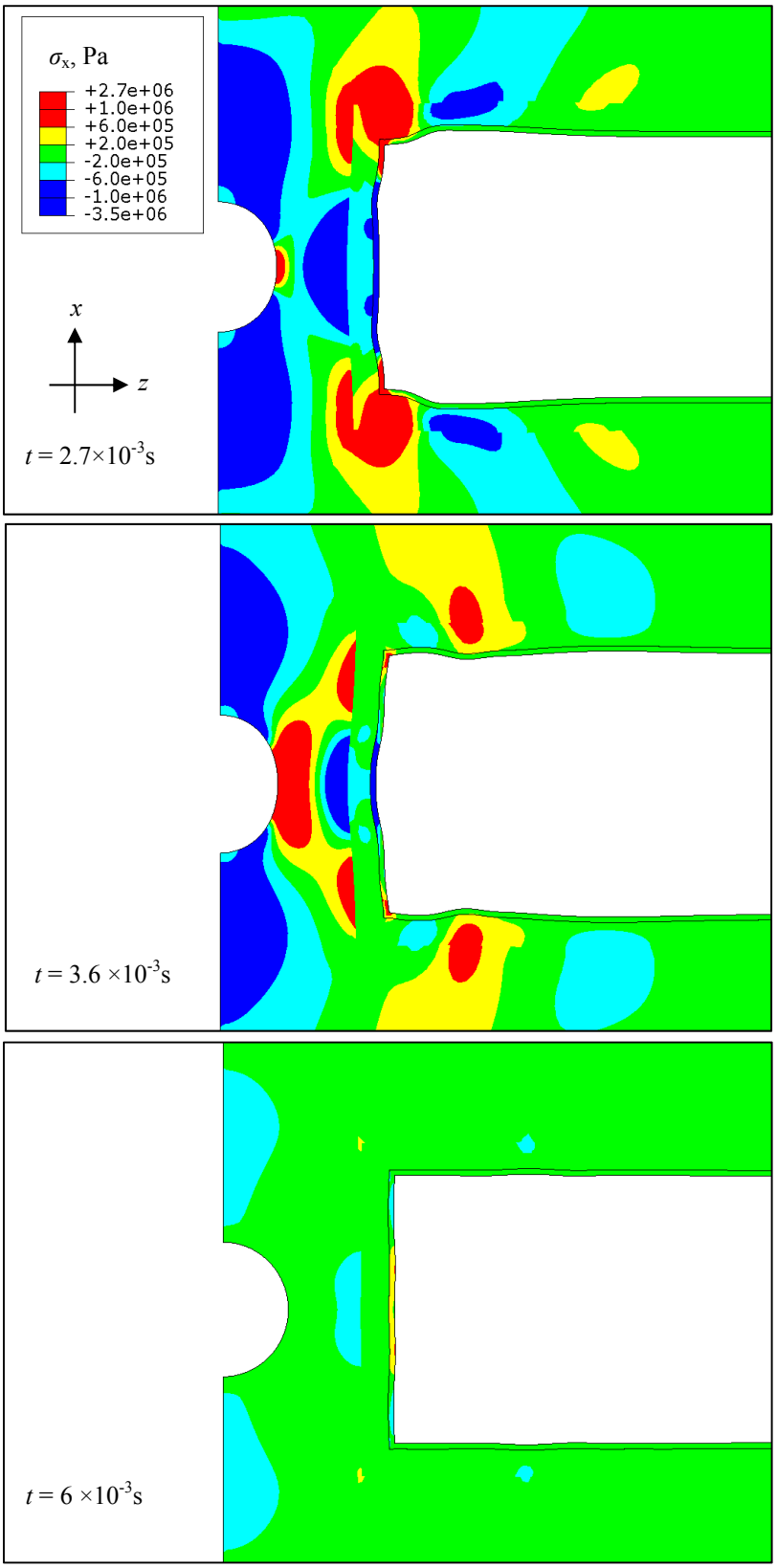

Figure 5.13: Contours of stresses in x-direction (σ_x) of the side walls of the tunnel. Deformation scale 1:1000.

A three-dimensional finite element model, of a set-up similar to what is used by Kwan et al. [75-76] in a laboratory test, is analysed with the Abaqus/Explicit solver [119]. The laboratory investigation is here described in Section 4.2 and in [Paper VI]. The model consists of a concrete prism of plain, unreinforced concrete and a steel hammer, as shown in Figure 5.14. The geometry of the concrete prism is the same as in [75-76], i.e. 100×100×500 mm^3, but for the hammer the dimensions where not given. For the following analysis, the hammer cross-section is assumed identical to that of the prism, giving a hammer of identical size as the prism, which, with a steel density of 7800 kg /m^3, weighs 39 kg, close to that of the hammer in the laboratory tests [75]. The model consists of 4300 nodes and 3200, 8-noded continuum elements with reduced integration (solid elements C3D8R) each with the size 15×15×15 mm^3. For more details, see [Paper VI].

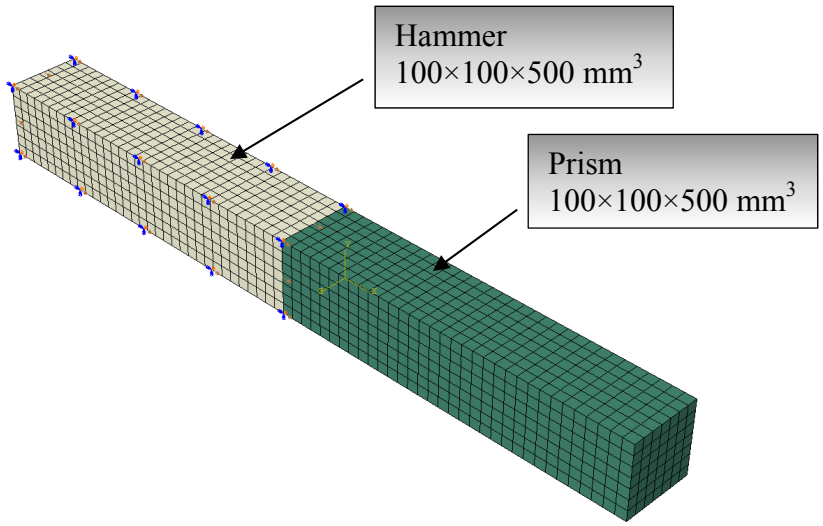

Figure 5.14: Finite element model of laboratory impact vibration test, from [Paper VI].

As outlined before, in the case of early age concrete subjected to impact excitation, cracks that develop completely under tensile stress are assumed the most important aspect of the behaviour, and that dominates the modelling. Several material models for concrete are implemented in most modern finite element analysis programs, e.g. Abaqus [120]. The brittle cracking model, adopted in the present study, is suitable for brittle failure of concrete and contains a minimal set of material constants, which can be estimated from data given in [Paper VI].

The damage criteria used in [Paper VI] assume that the initiation of damage occurs when loading conditions, e.g. impact loads, produce effective inelastic strains that exceed a certain threshold leading to cracking. This level is assumed to depend on the general state of stress in terms of crack width before formation of macro-cracks in one element or fracture zones within the concrete matrix, more detailed information described in [Paper VI]. It was observed that the free vibration modes of the test prisms contribute to strain concentrations that give cracking. For example in Figure 5.15(a), it can be seen that the maximum inelastic strain is located at three positions within the middle third of prism length, corresponding to the fourth mode shape. The simulated results give the PPV location plot and corresponding crack widths along the length of the prism of prism at 18 h concrete age as shown in Figure 5.16. Figure 5.16(a), demonstrates that with an impact velocity of 1500 mm/s, the PPV at a location of about 0.2 m from the impacted end reaches a high value, even higher than at

the end surface. This location is in good agreement with the position of experimentally observed cracks [76] and indicates that the mode shape of the free-free ended prism has significant influence on the initiation of cracks at these positions. The resonance frequencies are the distinct peaks, Figure 5.16(b), corresponding to the four free vibration modes of the free-free ended prism where the fourth mode is dominant [Paper VI]. The prism also shows cracks within the middle third along its length. A comparison shows that the maximum cracks and PPV levels represent a damaged section of the prism and that cracks and undamaged concrete between two cracks have a filtering effect on the propagation of impact vibration waves. It should be noted that the figure indicates one macro crack and three micro-cracks for the case with 1500 mm/s impact velocity. Therefore, it is important to investigate possible failure types and modes and the variation of these as concrete hardens. As an alternative, the models are modified with a notched at the middle section giving a predictable cracking behaviour. Thus, all the cracking will be concentrated to one wide crack, as shown in Figure 5.15(b).

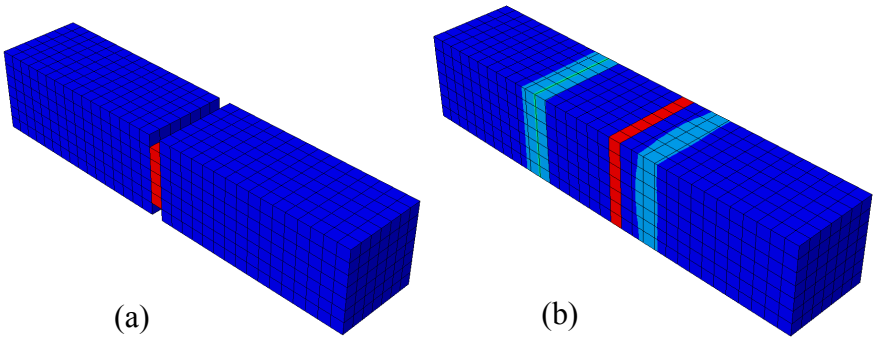

Figure 5.15: Inelastic strain of 8 h old prisms of concrete class C50. Impact velocity is 500 mm/s, for (a) notched prism and (b) un-notched prism, [Paper VI].

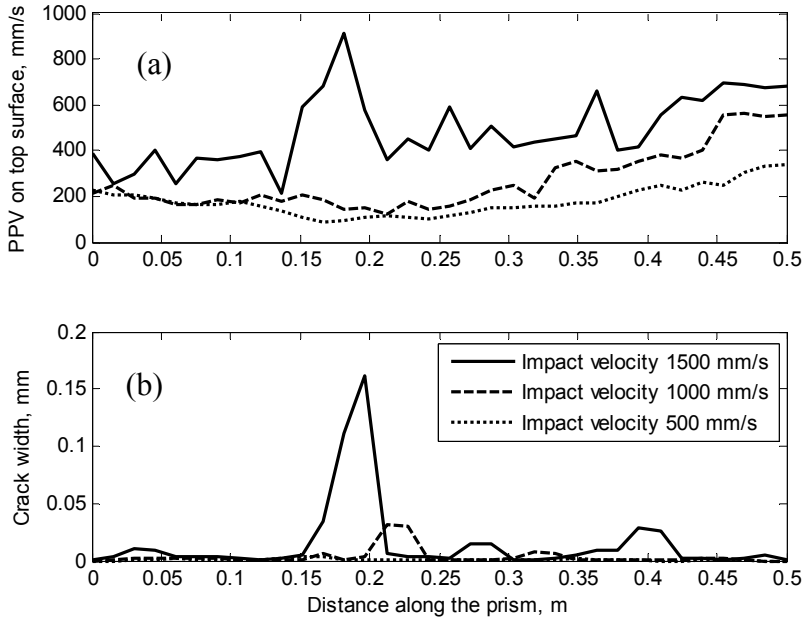

Figure 5.16: Concrete prism of age 18 hours, (a) Simulated PPV on top surface along the length of the prism, (b) Crack positions and magnitude along the length on the top surface of the prism.

Chapter 6

Summary of appended papers

Paper I: **Impact load vibrations on young concrete**

Anders Ansell, Lamis Ahmed. Submitted to Structural Concrete in April 2015.

Guidelines for allowable vibrations from impact-type loads on young and hardening concrete are of great value for civil engineering and concrete construction work. This paper summarizes important research within the field and comments on in situ observations and laboratory tests. The time after casting determines the concrete strength that must be reached to avoid damage and the allowed minimum distance from the source of vibration is related to the type of vibration activity and how the vibrations propagate towards the concrete. Most construction sites cover large areas and therefore guidelines for impact-type loads such as blasting, must be expressed in both time and distance. The large safety distances and time margins used today cause unnecessary delays thereby increasing building costs.

The paper provides a state-of-the art report on the field of impact vibrations on young and hardening concrete and gives a knowledge basis for the project. It is here suggested that concrete construction can be classified as either aboveground or underground (mass) concrete, or structural concrete, which is used to define the scope of this project.

Paper II: **Laboratory investigation of stress waves in young shotcrete on rock**

Lamis Ahmed, Anders Ansell (2012) Magazine of Concrete Research 64(10):899-908.

A non-destructive laboratory experiment with a concrete bar impact loaded by a hammer is presented in this paper. The test is set up to describe wave propagation through rock, here represented by the concrete bar, towards shotcrete on e.g. a tunnel surface. Cement based mortar with properties that resembles shotcrete was used and the properties of the bar is similar to that of rock. The stress wave propagation along the bar was registered using accelerometers, followed by finite element modelling to verify the test results.

The paper contributes with a description of the behaviour of young shotcrete under dynamic load, verifying previously recommended maximum allowed vibration velocities. It also shows how a laboratory model with an impacting hammer can be used to initiate the same type of stress waves that is the result of blasting in good quality rock, which is important also for the studies of cast concrete.

Paper III: **Structural dynamic and stress wave models for the analysis of shotcrete on rock exposed to blasting**

Lamis Ahmed, Anders Ansell (2012) Engineering structures 35(1):11-17.

This paper presents a comparison between numerical models describing stress wave propagation through rock as a result of blasting. The focus is on analysis methods to estimate the vibration vulnerability of young shotcrete. The interaction between shotcrete and rock and the stresses built up by propagating stress waves are described. The tested models are of two basic types, first finite element based structural dynamic models using concentrated masses, spring elements and elastic beams and secondly one-dimensional elastic stress wave models. The study connects previously presented analytical and in situ studies, demonstrating that structural dynamics and stress wave theory are two methods that can be used to describe the same response to impact-type vibration loads.

The contribution is here a demonstration that the two types of dynamic analysis methods give comparable results although the definition of the dynamic loads is different. The experience from numerical implementation of the load is used in the following development of analysis methods, based on 2D (and 3D) finite element formulations.

Paper IV: **Finite element simulation of shotcrete exposed to underground explosions**

Lamis Ahmed, Anders Ansell, Richard Malm (2012) Nordic Concrete Research (45):59-74.

A finite element analysis based on elastic material behaviour is presented. The models presented describe how stress waves from blasting propagate through rock and the stresses that develop when reaching a free surface covered by shotcrete, possibly leading to bond failure at the interface. The stress wave attenuation due to inhomogeneous rock characteristics, i.e. cracks, is included in the model. Age-dependent shotcrete material properties are used in the analysis in order to investigate the vulnerability to blast loading. Two cases of detonation close to a tunnel is investigated in 2D, side on impacts on a tunnel profile and stress waves approaching the face of a tunnel under construction, represented in the horizontal plane.

The paper is a continuation to Paper III, demonstrating how finite element models can be used for a 2D representation of stress propagation through hard rock, towards shotcrete. The numerical results are compared to the previous results using the structural dynamic and stress wave models. The implementation of material damping is also evaluated.

Paper V: **Vibration vulnerability of shotcrete on tunnel walls during construction blasting**

Lamis Ahmed, Anders Ansell (2014) Tunnelling and Underground Space Technology 42:105–111.

A case study based on measurements during tunnelling is presented. Earlier in situ measurements of vibrations on a shotcreted rock wall during tunnel excavation blasting is compared with numerical finite element results. The effect on shotcrete from blasting operations during tunnelling is studied, with focus on young and hardening shotcrete. The previously suggested model is here able to describe stress wave propagation in two dimensions, here also showing the importance of shear stresses at the rock-shotcrete interface. The vibration vulnerability of young shotcrete is investigated and it is also shown that distance and shotcrete thickness are important factors for how much time of waiting between spraying and blasting is needed.

This paper demonstrates how the finite element model developed and tested in Papers III-IV can be implemented for evaluation of in situ tunnel measurements. It connects numerical analysis methods and results with in situ measurements. It also adds important, additional measurement results for modelling verifications as a complement to the previous comparisons with the smaller scale in situ tests performed with blasting at closer distance in mining environment.

Paper VI: **Numerical modelling and evaluation of laboratory tests with impact loaded young concrete prisms**

Lamis Ahmed, Anders Ansell, Richard Malm. Submitted to Materials and Structures in April 2015.

Results from laboratory tests with impact loaded young concrete prisms are evaluated using a finite element model. The application of the dynamic load from an impacting hammer is used as with previously tested models, but here are 3D solid elements used. A non-linear material model is also implemented, capable of describing cracking during stress wave propagation. The position and width of cracks and measured particle vibration velocities are calculated and compared with the laboratory test results. Alternative geometry for the test prisms, with a notched section, is tested. This results in one wider crack at the centre of the prisms instead of two or three cracks distributed over its length. The geometry has been recommended for future laboratory test specimens since the appearance of cracks will become easier to detect, thus facilitating a more precise determination of critical vibration velocities. Finally, recommended damage limits for early age concrete are given, based on numerical calculations for two types of normal strength concrete.

The paper demonstrates the use of non-linear material representation together with the previously suggested finite element model. It also shows the implementation for modelling of cast concrete specimens, also using a 3D modelling approach.

Chapter 7

Recommendations

This chapter summarizes recommendations that are part of the conclusions from the project. At first, comments on practical aspects to be implemented in finite element modelling are given. Then follows a section that comments on the practical use and selection of the recommendations and guidelines summarized in chapter 3 and in the appended papers. The last section gives recommendations for further research, both with respect to analytical modelling and testing in situ and in laboratory environments.

7.1 Finite element modelling

For further development of finite element models and analysis of young concrete subjected to impact-type loads it is recommended that 2D models are used when the geometry of the surrounding ground is of importance, e.g. for reflection of stress waves. For more detailed studies of concrete elements a 3D analysis can be justified, especially if crack propagation is of interest, see [Paper VI]. In many cases, linear elastic material models can be used, making it possible to detect positions on the studied concrete structures where cracking will occur, or bond failure as in the case with shotcrete on rock. If there is a need to determine the extent of cracking, non-linear concrete material models should be introduced, but this will lead to much longer computational times and larger efforts. Impact loads such as from blasting or mechanically from a striking object can be introduced as a boundary condition in the model, e.g. as a velocity field. It should be noted that when modelling an impact from a striking object, e.g. a hammer, the impact velocity would be about twice that of the initial particle velocity propagating through the concrete, which is thoroughly discussed in [Paper III]. The load from a detonation inside a rock mass can be introduced by applying a velocity field on the perimeter of a circle surrounding the detonation point. The radius of the circle should be chosen so that the rock outside this area does not crack because of the detonation and with the correct velocity level calculated from a scaling relationship between vibration velocity, distance and weight of explosive charge.

7.2 Practical guidelines

When using and interpreting the guidelines for maximum allowed vibration velocities near young concrete, the type of concrete construction must be considered. The guidelines here

given in chapter 3 and accompanying papers, and in other referenced publications (see [Paper I]), relate primarily to mass concrete and conditions similar to that of load case (c) given in Figure 2.5. The vibration levels are not relevant to the case (a), structural concrete where the influence of mass and elastic properties require a specific structural dynamic analysis where the ground acceleration is possibly magnified by structural resonance. The focus is here on impact vibrations of short duration, but some of the published guidelines are based on continuous long-term vibration. It should therefore be noted that the guidelines presented and commented here are considered representative for short-term loads of high magnitude, and if applied to other cases, the duration of the load must be short. The project also included a comparison with the vibration resistance of shotcrete. Therefore, as a supplement recommendations also for this case are given, while e.g. sensitivity to bond failure between concrete and reinforcement have been excluded. The latter is related to load case (a) where the reinforcement configuration is complex and a structural dynamic analysis is required.

7.3 Further research

The further work must focus on establishing detailed guidelines for particular cases such as structural concrete, mass concrete above ground and underground and for shotcrete on rock. It is therefore important to investigate possible variations in failure types and modes with respect to the development of the material properties of hardening concrete. There is a great need for detailed parametric studies, including variation in concrete quality, hardening conditions, frequency content and variation with distance to the impact vibration source. More specialized load cases should also be investigated. An interesting example is blasting with multiple explosive charges where the least damaging sequence of detonation using different delay times is of interest. The suggested type of finite element models are useful for analysis work where a large number of parameter combinations can be efficiently tested. The models can be used for analysis of cases with various geometries in 2D and 3D, e.g. buried concrete structures such as slabs and footings and underground rock reinforcement structures of cast concrete and shotcrete. It will also be possible to model the reinforcing effect of bars, rock bolts, etc., in order to detect high, concentrated stresses where cracking and de-bonding may occur. Accurate analysis results will depend on reliable material data for young and hardening concrete, especially in the case with shotcrete where relatively little experimental work have been done and published. For both cast and sprayed concrete the time dependence for material properties such as compressive and tensile strengths, modulus of elasticity, shrinkage, creep and bond strength to reinforcement, other concrete structures and various rock types are of further interest. Dynamic laboratory testing on small scale test samples are of further use, for example with the modified test prism with notched sections here suggested in [Paper VI]. For further evaluation of the models and the obtained results more input from acceleration measurements are needed. Combining and comparing in situ measurements and observations with numerical modelling of the same cases will provide a good basis for reliable guidelines to be used for efficient civil and engineering work that involves activities that generate impact-type vibration close to young concrete structures and elements.

Chapter 8

Discussions and conclusions

The project has been interdisciplinary, combining structural dynamics, finite element modelling, concrete material technology, construction technology and rock support technology. After an initial project phase with focus on vibration and young shotcrete on hard rock the perspective has been widened also to include young, cast concrete. This has been possible since the analytical methods and models used have been applicable and possible to develop for both cases. The general scope of the project is thus young concrete and impact-type vibrations but it also includes a comparison between cast and sprayed concrete. In the following, the main conclusions are given, regarding load types, testing techniques, analysis techniques with respect to the similarities and differences between young cast and sprayed concrete.

8.1 Load type

A comparison between different dynamic loads that can act on young and hardening concrete shows that impact-type loads are by far the most serious, see [Paper I]. None of the other possible load types result in equally high load levels, expressed as either vibration velocity, acceleration or strain rate, see Figure 2.1 and 2.4. This load type is also characterized by relatively high frequencies and short duration. Typical impact loads are direct mechanical impacts, vibrations from blasting and e.g. seismic vibrations from earthquakes and dynamic fallout of rock masses due to high rock stresses. Pile driving is also regarded as an impact load but the stress propagation here usually takes place in soils softer than rock, which combined with common practical distance to concrete structures often leads to relatively low levels of vibration. Traffic loads often represent another type of load and can be classified as intermittent and of relatively long duration. However, uneven road surfaces can lead to impact-type loads during passage of heavy vehicles but these usually correspond to moderate intensities of vibrations. Damage that occurs during repair of bridges with passing traffic is due to relative displacements between old and new concrete sections and should thus be analysed with structural dynamics or quasi-static methods. In the analysis of the vibration sensitivity for concrete structures, clear definition of the case studied should be made with the choice of analysis methods based on this. For young concrete structures affected by impact loads, it is here recommended that a classification into three types is made; structural concrete, concrete aboveground and belowground concrete. For the first type, the natural frequencies and dynamic properties of the structure are critical and therefore a specific structural dynamic analysis must be performed in these cases. Here, an example is a newly

cast concrete slab supported by weak columns and possibly formwork structures. The situation of more compact concrete structures on the ground is equal to the case of earthquake loads resulting in inertial forces and rigid body displacements. The case with shotcrete on rock subjected to blasting vibration can be described in this way. The perhaps most important of the three cases, is structures below ground where impact waves can propagate directly into the concrete volume, see Figure 2.5, possibly resulting at high levels of vibration. These concrete structures are also confined and follow the movement of the surrounding soil or rock without relative deformation. Besides being the case for which the maximum vibration levels may appear, it is also the case where defined vibration limits will be most relevant.

8.2 Test results and measurement

In the case of in situ testing, blasting is the most common and relevant impact load type. Measurements associated with pile driving have also been performed but, as commented above, they often result in low vibration velocities, which in most cases are harmless to young concrete. However, for both of these load types the soil or ground properties are of great importance for the vibration propagation, from source of vibration towards concrete construction. Field experiments and observations with direct impacts against the concrete are not documented, except for certain types of tests to determine the energy absorption capacity, but these have been excluded here. No field measurements have been carried out within the project but results from previous and related projects were used to obtain relevant load data, to verify the analytical models and to conduct comparisons of results. In these cases the acceleration measurements were done during blasting in tunnels through hard rock, see Sections 4.3–4.4. When it comes to testing in laboratory environments, it is not practical to use explosives but traditionally vibratory loads have been produced by using a shaking table that provides long-lasting continuous vibration or impact loads from pendulum hammers or similar. The latter test method has been used in this project; see Section 4.1.1 and [Paper II]. The experiments were intended to investigate stress wave propagation through rock and towards bonding, young shotcrete. However, the acceleration measurements on the concrete beam used in the tests have not only been of great importance in the general modelling work but also for the understanding and interpretation of one-dimensional stress wave propagation in an elastic medium, from the application of the load to reflection at a free surface followed by superposition of waves. The test results have also been important as basic knowledge during the interpretation of other researchers' similar tests, here used in the evaluation process, see Section 4.2. Within the project, a further laboratory investigation was also done; see Section 4.1.2. These results were needed for the choice of Poisson's ratio for young concrete from the various results published by other researchers. The results indicate a wide variation during the first 12 hours followed by convergence towards the value that applies to fully hardened concrete.

8.3 Numerical modelling techniques

The work with evaluating and proposing analytical models has been performed in several steps, first with a focus on describing the behaviour of shotcrete on hard rock. First, less sophisticated structural dynamic models were examined, based on the finite element principle with lumped masses and spring elements. Elastic beam elements with distributed masses were also used. In addition, an elastic stress wave propagation model based on discrete elements

was tested. This one and the mass-spring analytical model are able to reproduce deformations in one direction only (1D), but in the model based on beam elements two-dimensional (2D) horizontal displacement planes can be calculated. The three models have been compared, see Section 5.1 and [Paper III], which resulted in the conclusion that their results are in good agreement, even though they are of different types and the dynamic impact loads are applied differently. The latter has led to important experiences for the following modelling work e.g. that if a dynamic load is applied as a boundary condition in the form of a velocity field the impact velocity onto a free surface must be double the resulting propagating particle velocity. This corresponds to an impact between two elastic bodies, e.g. a test rod and a hammer.

The model development continued with work to formulate a finite element model that enables displacement calculations in 2D, but with the ability to include more detailed geometries, see Sections 5.2.2–5.2.3. The model was based on linear elastic material properties as for the previously evaluated analytical models, for which good correspondence in the results was achieved, see [Paper IV]. Also in comparison with in situ measurements a high degree of accuracy was reached. First, a comparison was made with measurements from experiments in mining tunnels with ejected rock mass and shotcrete bond failure, see Sections 4.3, 5.2.2 and [Paper IV], and then with measurements made during blasting for tunnel construction where rock and shotcrete remained intact, see Sections 4.4, 5.2.3, and [Paper V]. The conclusion was that the elastic formulations were sufficient in these cases and that the previously tested principle of applying an impact load as a velocity field worked and gave realistic results. In addition to the study of shotcrete on vibration exposed hard rock, the modelling concept has also been used for the analysis of impact loaded beams and prisms of concrete modelled with 3D solid elements. In a first analysis, an elastic material model was used to validate laboratory experiments with hammer-loaded concrete beams, see Sections 4.1.1, 5.2.1, and [Paper II]. The laboratory beam remained un-cracked during the experiments, and thus it was possible to achieve good agreement using a linear elastic material model for fully hardened concrete. The model was further developed to enable modelling of cracked specimens. For verification results from earlier laboratory experiments with hammer impacted smaller prisms of young concrete were used, see Section 4.2. The comparison showed that the results from the laboratory tests can be reproduced numerically see Section 5.2.4 and [Paper VI]. The analysis showed that free vibration modes, and thus the natural frequencies, of the test prisms contributed to strain concentrations that gave cracking at high loads. Thus, the elastic material behaviour is decisive for location of the concrete damage in this case, as with shotcrete on rock and its bond failure. Furthermore, it was investigated how test prisms modified with notches at the middle section would behave during laboratory testing. Calculated results showed that all cracking here was concentrated to one crack with a width equal to the sum of the multiple cracks that develop in un-notched prisms. In laboratory testing, the modified prism with one wide crack provides a more reliable indication of the critical load level.

8.4 Concrete and shotcrete

The two cases of shotcrete on hard rock exposed to blasting and cast laboratory specimens subjected to direct impact load have been investigated using finite element models based on the same analysis principles. Stress wave propagation is described in the same way whether it is through hard rock towards a shotcrete lining or through a constructional element of young concrete. However, the failure modes differ for the two cases where shotcrete usually is damaged through loss of bond, partly or over larger sections that may result in shotcrete

falling down. Cracking in shotcrete is unusual and has not been observed during previous in situ tests, see Sections 4.3 and 4.4. For this reason, it is concluded that cracking of the shotcrete need not be described in the numerical analyses and that elastic material models may be used, which has also been shown to give good conformity with in situ test results, see Sections 5.2.2–5.2.3 and [Paper IV-V]. Because of the often symmetrical geometry of tunnels, the models can be implemented in 2D and thereby effectively be used when sections of the rock is included, also described as an elastic material. The observation plane can be positioned vertically for a study of a tunnel profile or horizontally to see the stress distributions along the walls of tunnels or caverns. As shown in the presented examples, crack formations closest to a rock surface exposed to blasting can be accounted for and so also damping during wave propagation through the rock. The latter gives a reduction in vibration velocity with increasing distance from the detonation point while rock cracks has a filtering effect on the frequency content. The main advantage here is that with the 2D geometry and elastic material behaviour, the model can effectively be implemented for whole tunnel sections that allows a representation of stress distributions that also includes reflections and superposition effects at sharp edges and corners. The model can thus provide a complete displacement field that includes the passage of P and S waves, and Rayleigh waves.

The study conducted for laboratory tested prisms of young concrete (see Section 4.2) differs from the case of shotcrete on rock mainly through the geometry and extent of the concrete volume. The shotcrete is to be seen as a relatively thin shell attached to a surface where wave propagation, reflection and superposition interact. The application of the load can be described by the three cases discussed in Section 2.4, where shotcrete on rock can be categorized as aboveground concrete while the prism case is more similar to the case of underground concrete where the impact load directly affects the concrete volume. Both types of concrete structures should however have been considered as mass concrete since they are reached by propagating stress waves. In the third case, structural concrete, it is the dynamic properties and resonance phenomena that interact with the ground motion. When damage occurs in the prisms exposed to impact loading, cracking takes place. The main conclusion from the numerical examples is that the free vibration modes of the prism interact, resulting in large stresses at some sections where cracks may be located. This is affected by the boundary conditions of the impacted element where a completely free element such as the prism will show cracks within the middle third along its length, in this case caused by the dominate fourth vibration mode, see Section 5.2.4 and [Paper VI]. Although this can be calculated with an elastic material model, as in the case of shotcrete, cracking and crack propagation must be described by non-linear concrete material models.

Vibration sensitivity of cast concrete and shotcrete has different critical ages because of the set accelerators used in the latter. Differences in temperature and humidity also play an important role for the cement hydration speed. When analysing the different cases the input in form of material parameters must reflect this, and preferably be based on in situ or laboratory testing. It is therefore not appropriate to e.g. use material data from testing of cast specimens in an analysis of vibration sensitivity of young shotcrete. The difference should also be considered when guidelines and recommendations are compiled, see Chapters 3 and 7. Mainly, the vibration resistance at early age is larger for a shotcrete lining than for a concrete volume extending in all three dimensions. An important factor is here the inertial forces that develop when concrete masses are accelerated by vibrations. Since the critical material property of shotcrete is the bond to the rock and its mass per unit area is low, the inertial forces become relatively small and the vibration resistance greater compared with a more homogeneous concrete volume. In the latter case, a concrete element can be pulled apart upon

passage of stress waves with cracking as a result. The dimensions of a concrete element in relation to the wavelength are also important with respect to reflection, superposition and build-up of stresses. Within a thin shotcrete, lining large stresses will not accumulate to the same extent as in an element with a length that is ten times longer or more.

Bibliography

References that only occur in Papers I-VI are marked with an asterisk followed by the papers roman numerals.

[1]. ACI Committee 116. Cement and concrete terminology, ACI 116R-90. Detroit, MI: American Concrete Institute; 1990.

[2]. Ahmed L. Models for analysis of shotcrete on rock exposed to blasting. Licentiate thesis. Stockholm: KTH Royal Institute of Technology; 2012.

[3]. Akins KP, Dixon DE. ACI SP-60-Concrete Structures and construction vibrations. Detroit, MI: American Concrete Institute; 1979,

[4]. Ansell A, Silfwerbrand J. The vibration resistance of young and early age concrete. Structural Concrete 4(3):125–134, 2003.

[5]. Ansell A. Dynamically loaded rock reinforcement. Doctoral thesis. Stockholm: KTH Royal Institute of Technology; 1999.

[6]. Ansell A. A Literature review on the shear capacity of dynamically loaded concrete structures. Stockholm: KTH Royal Institute of Technology, Concrete Structures. Report 89, 2005.

[7]. Ansell A. A Literature review on the vibration resistance of young and early age concrete. Stockholm: KTH Royal Institute of Technology, Concrete Structures. Report 68, 2002.

[8]. Ansell A. Dynamic finite element analysis of young shotcrete in rock tunnels. ACI Structural Journal 104(1):84-92, 2007.

[9]. Ansell A. In situ testing of young shotcrete subjected to vibrations from blasting. Tunnelling and Underground Space Technology 19(6):587-596, 2004.

[10]. Ansell A. Recommendations for shotcrete on rock subjected to blasting vibrations, based on finite element dynamic analysis. Magazine of Concrete Research 57(3):123-133, 2005.

[11]. Ansell A. Shotcrete on rock exposed to large-scale blasting. Magazine of Concrete Research 59(9):663-671, 2007.

[12]. Arora S, Dey K. Estimation of near-field peak particle velocity: A mathematical model. Journal of Geology and Mining Research 2(4):68–73, 2010.*V

[13]. Assessing vibration- A technical guideline. Sydney: NSW Department of Environment and Conservation; 2006.

[14]. ASTM C215-08. Standard test method for fundamental transverse, longitudinal, and torsional frequencies of concrete specimens. West Conshohocken, PA: ASTM International; 2008.

[15]. Aure TW, Ioannides AM. Numerical analysis of fracture process in pavement slabs. Canadian Journal of Civil Engineering 39(5):506-514, 2012. *VI

[16]. Barrett SVL, McCreath DR. Shotcrete support design in blocky ground: towards a deterministic approach. Tunnelling and Underground Space Technology 10(1):79–89, 1995. *V

[17]. Bastian CE. The effect of vibrations on freshly poured concrete. Foundation Facts 6(1):14-17, 1970.

[18]. Bieniawski, Z. Determining rock mass deformability: Experience from case histories. International Journal of Rock Mechanics and Mining Sciences 15(5):237–247, 1978. *IV,V

[19]. Bischoff PH, Perry SH. Compressive behaviour of concrete at high strain rates. Materials and Structures 24(6):425-450, 1991.

[20]. Bonzel J, Schmidt M. Effects of shocks on fresh and new concrete. Beton 30(9): 333-337, 1980. *I

[21]. Brandl H, Günzler J. Einfluss von Erschütterungen im frühen Erhärtungsstadium von Beton auf den Haftverbund mit Stahl (In German). Bauplanung-Bautechnik 43(1):13-16, 1989. *I

[22]. Bro2002. Swedish Road Administration (in Swedish). Borlänge: Vägverket Publ 2002:47; 2002. *I

[23]. Bro2004. Swedish Road Administration (in Swedish). Borlänge: Vägverket, Publ 2004:56; 2004.

[24]. Brown DA, Turner JP, Castelli RJ. Drilled shafts: Construction procedures and LRFD design method. Washington DC: Federal Highway Administration. Report FHWA NHI-10-016, 2010. *I

[25]. Bryne L-E, Ansell A, Holmgren J. Laboratory testing of early age bond strength of shotcrete on hard rock. Tunnelling and Underground Space Technology 41:113-119, 2014. *V

[26]. Bryne L-E, Holmgren J, Ansell A. Experimental investigation of the bond strength between rock and hardening sprayed concrete. Proceedings of the 6th International Symposium on Sprayed Concrete. Tromsø: Norwegian Concrete Society, , 2011. *II,IV

[27]. Bryne L-E. Time dependent material properties of shotcrete. Doctoral thesis. Stockholm: KTH Royal Institute of Technology; 2014.

[28]. BS 7385-2:1993. Evaluation and measurement for vibration in buildings – Part 2: Guide to damage levels from groundborne vibration. London: British Standards Institution; 1993. *I

[29]. Byfors J. Plain concrete at early ages. Stockholm: Swedish Cement and Concrete Institute; 1980.

[30]. Chang Y. Tunnel support with shotcrete in weak rock - A rock mechanics study. Doctoral thesis. Stockholm: KTH Royal Institute of Technology; 1994. *IV,V

[31]. Chen M, Lu WB. Research on safety vibration velocity for reshly mixed concrete of dam foundation under loading of blasting vibration. Journal of Wuhan University of Technology-Mater. Sci. Ed. 37(2):4-9, 2004. *I
[32]. Clough RW, Penzien J. Dynamics of structures. New York: McGraw-Hill; 1993.*III
[33]. Cusson D, Repette W L. Early-age cracking in reconstructed concrete bridge barrier walls. ACI Material Journal 97(4):438-446, 2000. *I
[34]. DIN 4150-3:1999-02. Vibrations in buildings - Part 3: Effects on structures. Berlin: Deutsches Institut für Normung; 1999. *I
[35]. DL/T5135-2001. Chinese professional standard - Technical code of construction of engineering blasting of hydropower structures. Beijing: Water Resources and Electric Power; 2001. *I
[36]. Dowding CH. Construction vibrations. Upper Saddle River, NJ: Prentice-Hall; 1996.
[37]. Dunham MR, Rush AS, Hanson JH. Effects of induced vibrations on early age concrete. Journal of Performance of Constructed Facilities 21(3):179-184, 2007. *I
[38]. Dunham MR, Rush AS, Hanson JH. Parametric analysis of the effects of induced vibration on concrete early ages. Terre Haute IN: Engineering Forensic Research Institute. Repot EFRI04/A01, 2004. *I
[39]. EN 12390-3:2009. Testing hardened concrete - Part3: Compressive strength of test specimens. Brussels: European Committee for Standardisation (CEN); 2009. *VI
[40]. EN 1992-1-1. Eurocode 2 Design of concrete structures- Part 1-1: General rules and rules for buildings. Brussels: European Committee for Standardisation (CEN); 2004.
[41]. Esteves JM. Control of vibration caused by blasting. Lisbon: Laboratorio de Engenharia Civil; 1978.
[42]. Fjellström P, Jonasson J-E. Emborg M., Hedlund H. Model for concrete strength development including strength reduction at elevated temperatures. Nordic Concrete Research 45: 25-44, 2012.
[43]. Forrestal MJ, Togami TC, Baker WE, Frew DJ. Performance evaluation of accelerometers used for penetration experiments. Experimental Mechanics 43(1):90–96, 2003. *II
[44]. Freyne SF, Watkins ML. Acceptable vibrations on green concrete. Jackson MS: Mississippi Department of Transportation. Report MS-DOT-RD-13-252, 2013.
[45]. Furr HL, Fouad FH. Bridge slab concrete placed adjacent to moving live load. Texas: Texas Transportation Institute, Texas A&M University, College Station TX. Research Report 266-1F, 1981. *I
[46]. Gamble DL, Jow Y-K, Simpson TA. Effects of blasting vibrations on uncured concrete foundations. Proceedings of the 11th Conference on Explosives and Blasting Techniques. Cleveland OH: International Society of Explosives Engineers; 1985. *I
[47]. Gao Z, Zhu Q, Huang X, Huang X. Experimental research and numerical analysis of the effects of blasting vibration on young concrete. Proceeding of 12th COTA International Conference of Transportation Professionals. Beijing: Multimodal Transportation Systems - Convenient, Safe, Cost-Effective, Efficient, CICTP 2012; 2012.
[48]. GB6722–2003. Safety regulations for blasting, Beijing: Chinese Society of Engineering Blasting; 2013. *I

[49]. GB6722-2011. Safety regulations for blasting. Beijing: Chinese Society of Engineering Blasting; 2011. *I
[50]. Goel MD, Matsagar VA. Blast-resistant design of structures. Practice Periodical on Structural Design and Construction 19(2):1-9, 2014.
[51]. Graff KF. Wave motion in elastic solids. NewYork: Dover Publications; 1975. *II
[52]. Gustafsson P. Fracture mechanics studies of non-yielding materials like concrete: modelling of tensile fracture and applied strength analysis. Lund: Division of Building Materials, University of Lund. Report TVBM-1007, 1985. *VI
[53]. Hahn T, Holmgren J. Adhesion of shotcrete to various types of rock surfaces and its influence on the strengthening function of shotcrete when applied on hard jointed rock. Proceedings of the 4th International Congress on Rock Mechanics. Montreux: International Society for Rock Mechanics; 1979.*III,V
[54]. Harsh S, Darwin D. Traffic-induced vibrations and bridge deck repairs. Concrete International 8(5):36-42, 1986.
[55]. Heiniö M. Rock excavation handbook. Helsinki: Sandvik Tamrock Corp; 1999.
[56]. Hillerborg A, Modéer M, Peterson P-E. Analysis of crack formation and crack growth in concrete by means of fracture mechanics and finite elements. Cement and Concrete Research 6(6):773-781, 1976. *VI
[57]. Hilsdorf HK, Brameshuber W. Code-type formulation of fracture mechanics concepts for concrete. International Journal of Fracture 51: 61-72, 1991. *VI
[58]. Holmberg R, Persson PA. The Swedish approach to contour blasting. Proceedings of 4th Conference on Explosive and Blasting Techniques. New Orleans: Society of Explosives Engineers; 1979. *V
[59]. Holmgren BJ. Shotcrete research and practice in Sweden – Development over 35 years. Proceedings of the 3th International Conference on Engineering Developments in Shotcrete. Queenstown: Australian Shotcrete Society and the American Shotcrete Association; 2010.*IV
[60]. Hong S, Park S-K. Effect of vehicle-induced vibrations on early-age concrete during bridge widening. Construction and Building Materials 77(15):179-186, 2015. *I
[61]. Hows EUV. Effects of blasting vibrations on curing concrete. Proceedings of the 20th United States Symposium on Rock Mechanics. Texas: American Rock Mechanics Association; 1979.
[62]. Huang LX, Chen YB. Rock dynamics in china: past, present and future (in Chinese). Chinese Journal of Rock Mechanics and Engineering 22(11):1887-1891, 2003. *I
[63]. Hulshizer AJ, Desai AJ. Shock vibration effects on freshly placed concrete. Journal of Construction Engineering and Management 110 (2):266-285, 1984.
[64]. Hulshizer AJ. Acceptable shock and vibration limits for freshly placed and maturing concrete. ACI Material Journal 93(6):524-533, 1996.
[65]. International Federation for Structural Concrete. *fib* Model code for concrete structures 2010. Lausanne: Wilhelm Ernst & Sohn, 2013.
[66]. Issa MA. Investigation of cracking in concrete bridge decks at early ages. Journal of Bridge Engineering 4(2):116–24, 2003.
[67]. James G. Modelling of young shotcrete on rock subjected to shock wave. Master thesis. Stockholm: KTH Royal Institute of Technology; 1998.

[68]. Jinnerot M, Nilsson H. Experimental study of shock wave propagation and damage zone determination during mining excavations (in Swedish: Experimentell studie av stötvågsutbredning och skadezonsberäkning vid ortdrivning). Master thesis. Gothenburg: Chalmers University of Technology; 1998. *V

[69]. Kendorski FS, Jude CV, Duncan WM. Effect of blasting on shotcrete drift linings. Mining Engineering 25(12):38-41, 1973.

[70]. Kinsler LE, Frey AR, Coppens AB, Sanders JV. Fundamentals of acoustics. New York: Wiley; 1993. *II

[71]. Klink SA. Aggregates, elastic-modulus, and Poisson's ratio of concrete. ACI Journal 83(6):961-956, 1986.

[72]. Krell WC. The effect of coal mill vibration of fresh concrete. Concrete International 1(12):31-34, 1979.

[73]. Kwan AKH, Lee PKK. A study of the effects of blasting vibration on green concrete. Hong Kong: Geotechnical Engineering Office, The government of the Hong Kong special administrative region. Geo Report No. 102, 2000.

[74]. Kwan AKH, Lee PKK. Testing the shock vibration resistance of concrete for setting vibration control limits against blasting damage. Proceedings of the 27th Conference on Our World in Concrete & Structures. Singapore: Singapore Concrete Institute; 2002. *I

[75]. Kwan AKH, Zheng W, Lee PKK. Shock vibration test of concrete. ACI Material Journal 99(4):361-370, 2002.

[76]. Kwan AKH, Zheng W, Ng IYT. Effects of shock vibration on concrete. ACI Material Journal 102(6):405-413, 2005.

[77]. Kwan KH, Ng PL. Effects of traffic vibration on curing concrete stitch: Part I - test method and control program. Engineering Structures 29(11):2871-2880, 2007. *I

[78]. Larnach WJ. Changes in bond strength caused by re-vibration of concrete and the vibration of reinforcement. Magazine of Concrete Research 4(10):17-21, 1952. *I

[79]. Leppänen J. Concrete structures subjected to fragment impacts - Dynamic behaviour and material modelling. Doctoral thesis. Gothenburg: Chalmers University of Technology; 2004.

[80]. Lou JW, Xu QJ, Long Y. Research on threshold for influence of blasting vibration velocity over the fresh concrete quality of the nuclear power station (in Chinese). World Information on Earthquake Engineering 19(2):163-167, 2003. *I

[81]. Lu W, Luo Y, Chen M, Shu D. An introduction to Chinese safety regulations for blasting vibration. Environmental Earth Sciences 67(7):1951-1959, 2012. *I

[82]. Lu WB. Determination of the limit of the safety velocity for young foundation concrete under blasting vibration loading (in Chinese). Explosion and Shock Waves 22(4):327-332, 2002. *I

[83]. MacInnis C, Kosteniuk PW. Effectiveness of revibration and high-speed slurry mixing for producing high-strength concrete. ACI Journal 76(12):1255-2365, 1979. *I

[84]. Magnusson J. Structural concrete elements subjected to air blast loading. Licentiate thesis. Stockholm: KTH Royal Institute of Technology; 2007.

[85]. Malm R. Predicting shear type crack initiation and growth in concrete with non-linear finite element method. Doctoral thesis. Stockholm: KTH Royal Institute of Technology; 2008. *VI

[86]. Malmgren L. Shotcrete rock support exposed to varying load conditions. Licentiate thesis. Luleå: Luleå University of Technology; 2001.[*III]

[87]. Malvar LJ, Crawford JE. Dynamic increase factors for concrete. Proceedings of the 28th DoD Explosives Safety Seminar Held in Orlando. Orlando, FL: Naval Facilities Engineering Service Centre; 1998.

[88]. Manning DG. Effects of traffic-induced vibrations on bridge-deck repairs. Washington DC: Transportation Research Board. NCHRP Synthesis No. 86, 1981.

[89]. Mascarenhas MF, Spillmann CM, Linder JF, Jacobs DT. Hearing the shape of a rod by the sound of its collision. American Journal of Physics 66(8):692–697, 1998.[*II]

[90]. Mathworks. Matlab. < http://www.mathworks.com/products/matlab/ >.[*II,III,VI]

[91]. McCreath DR, Tannant DD, Langille CC. Survivability of shotcrete near blasts. In: Rock Mechanics. Rotterdam: Balkema; 1994. [*II,III,V]

[92]. Mesbah HA, Lachemi M, Aitcin P-C. Determination of elastic properties of high-performance concrete at early ages. ACI Material Journal 99(1):37-41, 2002.

[93]. Meyers MA. Dynamic behaviour of materials. NewYork: John Wiley & Sons, 1994.[*II,III]

[94]. Mississippi Standard Specifications for Road and Bridge Construction. Jackson, MI: Mississippi Department of Transportation; 2004. [*I]

[95]. Muller-Rochhotz JFW. Traffic vibration of a bridge deck and hardening of lightweight concrete. Concrete International 8(11):23-26, 1986.

[96]. Nagy A. Determination of E-modulus of Young concrete with nondestructive method. Journal of Materials in Civil Engineering 9(1): 15-20, 1997.

[97]. Nakano N, ‘Okada S, Furukawa K, Nakagawa K. Vibration and cracking of tunnel lining due to adjacent blasting (in Japanese, Abstract in English). Proceedings of the Japan Society of Civil Engineers. Rombun-Hokokushu; 1993.

[98]. Neville AM. Properties of concrete. London: Prentice-Hall; 2010

[99]. Ng PL, Kwan AKH. Effect of traffic vibration on curing concrete stitch: Part II-cracking, debonding and strength reduction. Engineering Structures 29 (11):2881-2892, 2007.

[100]. Nihal Arıoglu Z, Girgin C, Arıoglu E. Evaluation of ratio between splitting tensile strength and Compressive Strength for Concretes up to 120 MPa and its Application in Strength Criterion. ACI Material Journal 103(1):18-24, 2006. [*VI]

[101]. Nilsson C. Modelling of dynamically loaded shotcrete. Master thesis. Stockholm: KTH Royal Institute of Technology; 2009.[*III]

[102]. NS 8141-1:2012/A1:2013. Vibration and shock - Guideline limit values for construction work, open-pit mining and traffic - Part 1: Effect of vibration and air blast from blasting on constructions, including tunnels and rock caverns (in Norwegian). Oslo: Standards Norway; 2013. [*I]

[103]. Nyström U. Modelling of concrete structures subjected to blast and fragment loading. Doctoral thesis. Gothenburg: Chalmers University of Technology; 2013.

[104]. Olofesson SO. Applied explosives technology for construction and mining. Sweden: Applex, Ärla; 1988.

[105]. Oluokun FA, Burdette EG, Deatherage JH. Elastic modulus, Poisson's ratio and compressive strength relationship at early ages. ACI Journal 88(1):3-10, 1991.

[106]. Oluokun FA, Burdette EG, Deatherage JH. Splitting tensile strength and compressive strength relationships at early ages. ACI Material Journal 88(2): 115-121, 1991. *VI
[107]. Oluokun FA. Prediction of concrete tensile strength from its compressive strength: Evaluation of existing relations for normal weight concrete. ACI Material Journal 88(3):302-309, 1991. *VI
[108]. Oriard LL, Coulson J H. TVA blast vibration criteria for mass concrete. Proceeding Conference of ASCE. Portland, OR: Preprint; 1980.
[109]. Oriard LL. Blasting effects and their control, handbook of underground mining methods. Englewood OH: Society of Mining Engineers of AIME; 1982. *I
[110]. Paz M. Structural Dynamics. Theory and computation. New York: Van Nostrand Reinhold; 1991.*III,IV
[111]. Persson P-A. The Relationship between Strain Energy, rock Damage, fragmentation, and throw in rock blasting. Fragblast - International Journal of Blasting and Fragmentation 1(1):99-110, 1997.
[112]. Petersson P-E. Crack growth and development of fracture zones in plain concrete and similar materials. Lund: Division of Building Materials, University of Lund. Report TVBM-1006, 1981. *VI
[113]. Reidarman L, Nyberg U. Blast vibrations in the Southern Link tunnel - Importance for fresh shotcrete? (in Swedish: Vibrationer bakom front vid tunneldrivning i Södra Länken - Betydelse för nysprutad betong?). Stockholm: Rock Engineering Research Foundation. SveBeFo-report 51, 2000.
[114]. Reinhardt HW. Concrete under impact loading, tensile strength and bond. Heron 27(3) Delft University of Technology, the Netherlands, 1982.
[115]. Revey GF. Managing rock blasting work in urban environments. Practice Periodical on Structural Design and Construction 11(2): 86-92, 2006.
[116]. RILEM commission 42-CEA. Properties of set concrete at early ages state-of-the-art-report. Materials and Structures 14(6):399-450, 1981.
[117]. Rinehart JS. On fractures caused by explosions and impacts. Quarterly of the Colorado school of mines, Golden 55(4): 1–115 1960.*II
[118]. Silfwerbrand J. The Influence of traffic-induced vibrations on the bond between old and new concrete. Stockholm: KTH Royal Institute of Technology; 1992.*III
[119]. Simulia, Abaqus user's examples and theory manual, version 6.12.
[120]. Simulia: < http://www.simulia.com/products/abaqus_explicit.html >; 2014.
[121]. Siwula J, Helwany S, Richard L. Construction vibration attenuation with distance and its effect on the quality of early age concrete. Milwaukee: Wisconsin Highway Research Program. Report WHRP 11-02, 2011.
[122]. SL47-94. Chinese professional standard - Technical code of construction of excavation of rock foundation of hydraulic structures. Beijing: Water Resources and Electric Power; 1994. *I
[123]. SS-4604866:2011. Vibration and shock: Guidance levels for blasting-induced vibration in buildings (in Swedish). Stockholm: SIS Swedish Standards Institute; 2011. *I
[124]. SS-ISO 4866:2010. Mechanical vibration and shock - Vibration of fixed structures: Guidelines for the measurement of vibrations and evaluation of their effects on structures. Stockholm: SIS Swedish Standards Institute; 2010. *I

[125]. Standards Norway. Vibrations from blasting and other civil engineering activities - Comments to NS 8141-1:2012+A1 and NS 8141-2:2013, P-741, Oslo, Norway, 2014. *I
[126]. Sun X, Sun J. Research on the damage fracture of rock blasting based on velocity response spectrum. Applied Mechanics and Materials 105-107:1521-1527, 2012.*IV
[127]. Swedish Concrete Association handbook to Eurocode 2, Vol. I-II (in Swedish). Stockholm: Swedish Concrete Association; 2012. *VI
[128]. Swedish Concrete Handbook. Betonghandbok–Material. Stockholm: AB Svensk Byggtjänst; 1994.
[129]. Tawfiq K, Mtenga P, Sobanjo J. Effect of construction Induced Vibrations on Green concrete in drilled shafts. Journal of Materials in Civil Engineering 22(6):637-642, 2010. *I,VI
[130]. Thomson WT. Theory of Vibration with Applications. Englewood Cliffs, NJ: Prentice hall; 1993.*II
[131]. TRVK Bro 11. Swedish Transport Administration (in Swedish). Borlänge: TRV publ nr 2011:085; 2011. *I
[132]. Tunnel 99. Swedish Road Administration (in Swedish). Borlänge: Vägverket Publ 1999:138; 1999.
[133]. Utsi S, Jonasson J-E. Influence of different amount of fly ash for early age concrete containing Swedish cement - Part I: Tendency model for heat and strength development for variable fly ash content. Nordic Concrete Research 41: 77-91, 2010.
[134]. Vandewalle M. Dramix – Tunnelling the world: with 7 reference projects. Zwevegem: NV Bekaert SA; 1998.*III
[135]. Wood DF, Tannant DD. Blast damage to steel fibre reinforced shotcrete. In: Fibre-reinforced Concrete – Modern Developments. Vancouver: University of British Columbia UBC Press, 1994.
[136]. Worsey P, Giltner SG, Drechsler T, Ecklecamp R, Inman R. Formulation of production blasting criteria for the construction of a lime plant at a major crushed stone operation. FRAGBLAST - International Journal for Blasting and Fragmentation 2(2):181-194, 1998. *I
[137]. Zhang C, Hu F, Zou S. Effects of blast induced vibrations on the fresh concrete lining of a shaft. Tunnelling and Underground Space Technology 20(4):356-361, 2005. *I
[138]. Zhu CT, Zhang ZY, Tong JY, Mei JY. Study on the influence of blasting on freshly placed concrete and its control standards (in Chinese). Blasting 7(3):28-32, 1990. *I